Article

Not peer-reviewed version

Genetic Modeling of Lysosomal Storage Disorders (LSDs), in the Brain-Midgut Axis of *Drosophila melanogaster*, During Aging

Sophia P. Markaki , Nikoleta-Joana Kiose , Zoi Charitopoulou , Stylianos Kougioumtzoglou , Athanassios D. Velentzas [*,†] , Dimitrios J. Stravopodis [*,†]

Posted Date: 21 November 2025

doi: 10.20944/preprints202511.1571.v1

Keywords: aging; brain; Drosophila melanogaster; Fabry disease; GAL4/UAS; gaucher disease; hunter syndrome; hurler syndrome; midgut; niemann-pick disease; pompe disease; RNAi; sly disease; Tay-Sachs/Sandhoff disease(s)

 doi:10.20944/preprints202511.1571.v1

Article

Genetic Modeling of Lysosomal Storage Disorders (LSDs), in the Brain-Midgut Axis of *Drosophila melanogaster*, During Aging

Sophia P. Markaki, Nikoleta-Joana Kiose, Zoi Charitopoulou, Stylianos Kougioumt oglou, Athanassios D. Velentzas *,† and Dimitrios J. Stravopodis *,†

Section of Cell Biology and Biophysics, Department of Biology, School of Science, National and Kapodistrian University of Athens (NKUA), 157 01, Athens, Greece

* Corresponding authors: tveletz@biol.uoa.gr (A.D.V.); dstravop@biol.uoa.gr (D.J.S.)

† These authors contributed equally to this work.

Abstract

Lysosomal Storage Disorders (LSDs) are a group of rare inherited diseases caused by mutations in genes encoding proteins involved in normal lysosomal functions, leading to accumulation of undegraded substrates within lysosomes. Among the most prominent clinical features are neurological impairment and neurodegeneration, arising from widespread cellular dysfunction. Development of powerful and reliable animal-model systems that can *in vivo* recapitulate human LSD pathologies is critical for understanding disease mechanisms and advancing therapeutic strategies. In this study, we identified *Drosophila melanogaster* orthologs of human LSD-related genes using the DIOPT tool and performed tissue-specific gene silencing along the brain-midgut axis via engagement of GAL4/UAS and RNAi combined technologies. Transgenic fly models were presented with key features of human LSD pathologies, including significantly shortened lifespan and progressive locomotor decline that serves as measure for neuromuscular disintegration, following age- and sex-dependent patterns. These phenotypic parallels in pathology strongly support the functional relevance of the selected orthologs and underscore the value of *Drosophila* as a versatile, *in vivo*, model system for advanced LSD-pathology research, offering state-of-the-art genetic tools for molecularly dissecting disease mechanisms, and providing cutting-edge novel platforms for high-throughput genetic and/or pharmacological screening, towards development of therapeutically beneficial, new, drug-based regimens and mutant gene-rescue schemes.

Keywords: aging; brain; *Drosophila melanogaster*; Fabry disease; GAL4/UAS; gaucher disease; hunter syndrome; hurler syndrome; midgut; niemann-pick disease; pompe disease; RNAi; sly disease; Tay-Sachs/Sandhoff disease(s)

1. Introduction

Lysosomal Storage Disorders (LSDs) are a group of rare diseases comprising more than 70 inherited metabolic disorders that are being characterized by lysosomal dysfunction and subsequent accumulation of undegraded substrates within lysosomes. LSDs are monogenic diseases caused by alterations in genes encoding proteins involved in normal lysosomal function, such as lysosomal enzymes and lysosomal membrane proteins, and their combined prevalence is estimated to be approximately 1 in 8,000 live births [1–4].

Lysosomal impairment leads to the dysregulation of a diverse range of cellular processes being associated with lysosomes, such as membrane repair, vesicle trafficking, lipid homeostasis, signaling, cell death pathways, autophagic flux and clearance of autophagosomes. Therefore, autophagic impairment has been described as a common mechanism of pathology in an increasing number of LSDs [4–6]. Despite their heterogeneity, their major clinical symptoms include hepatosplenomegaly,

 doi:10.20944/preprints202511.1571.v1

pulmonary and cardiac disorders, skeletal abnormalities and -often- central nervous system (CNS) dysfunction, with patients being frequently presented with a progressive neurodegenerative clinical course [6,7]. Typically, LSDs are primarily classified according to the biochemical properties of the accumulated undegraded substrate, and include sphingolipidoses, glycogen storage diseases and mucopolysaccharidoses [4,8].

Sphingolipidoses are disorders caused by genetic defects in the catabolism of sphingosine-containing lipids, and their accumulation affects both the CNS and peripheral organs [9]. Gaucher, Fabry, Tay-Sachs and Niemann-Pick are classified among the most common sphingolipid metabolism diseases [8–10]. Gaucher disease (GD), which is subdivided into three different types, is the most prevalent form of sphingolipidoses, and is caused by mutations in the *GBA* gene, which encodes for the lysosomal hydrolase β-Glucocerebrosidase, responsible for the degradation of glucosylceramide into glucose and ceramide [4,8–10]. Fabry, an inherited X-linked disease, is the second most common form of sphingolipidoses [2], and is caused by mutations in the *GLA* gene encoding the enzyme α-Galactosidase A, which catalyzes the lysosomal hydrolysis of globotriaosylceramide [4,7,10]. Tay-Sachs, a type of GM2 gangliosidosis, is presented with severe neurological symptoms and is caused by mutations in the *HEXA* gene encoding the enzyme β-Hexosaminidase A, which is responsible for breaking down GM2 gangliosides, resulting in their toxic accumulation in neuronal tissues [11]. Niemann-Pick is a group of predominantly neurodegenerative disorders classified in types A and B, caused by mutations in the *SMPD1* gene, while type C derives from mutations in the *NPC1* or *NPC2* genes. In types A and B, the affected enzyme is the Sphingomyelinase (ASM), leading to sphingomyelin buildup, whereas in Niemann-Pick type C, proteins that mediate cholesterol transport from endosomes/lysosomes are seriously affected, causing endo-lysosomal accumulation of cholesterol, glycosphingolipids and sphingomyelin, resulting in severe neurological pathology [1,6,12].

Glycogen storage diseases (GSDs) comprise a group of inherited metabolic disorders caused by mutations in genes encoding enzymes of glycogen metabolism. Among them, Pompe disease, also known as GSD II, is classified as a major LSD family member. Pompe disease results from mutations in the *GAA* gene encoding α-Glucosidase, which is a key lysosomal enzyme responsible for the hydrolysis of glycogen to glucose. The hallmark of Pompe disease is glycogen accumulation in lysosomes, predominantly in muscle cells, leading to cardiorespiratory failure [4,7,8].

Mucopolysaccharidoses (MPSs) form a group of eleven LSD pathologies, characterized by the cellular accumulation of glycosaminoglycans (GAGs), which are negatively charged polysaccharides essential for several cellular processes, including signaling and development. The classification of MPSs is based on mutations in specific enzymes that catabolize target substrates, with MPS I, II and III being the most common ones [4]. MPS type I (MPS I) is caused by the deficiency of lysosomal hydrolase α-L-Iduronidase (IDUA), leading to the accumulation of dermatan- and heparan-sulfate inside lysosomes of a wide range of tissues. The severe form of MPS I, known as Hurler syndrome, is characterized by early onset, and progressive somatic and neurological impairments [13]. MPS II, also known as Hunter syndrome, is caused by mutations in the *IDS* gene on the X chromosome and is typically described by neurological deterioration. These mutations result in a critical deficiency of Iduronate-2-sulfatase (IDS), an enzyme responsible for breaking down dermatan- and heparan-sulfate. Finally, Sly disease, also known as MPS VII, is caused by mutations in the *GUSB* gene, resulting in β-Glucuronidase (GUSB) enzyme deficiency. This leads to the accumulation of dermatan-, heparan- and chondroitin-sulfate GAGs, causing progressive multi-system dysfunctions [4,14].

Neurological dysfunction and progressive neurodegeneration are key symptoms of LSDs [6]. The study of -animal- model organisms is imperative for advancing our understanding of human pathologies, thus enabling the identification of novel disease-related pathways that have the potential to serve as drug targets. Furthermore, recent progress has led to development of more powerful and reliable animal models that can more precisely mirror aberrant phenotypes and pathological processes of human diseases and, in particular, LSDs [15–17]. A recently explored therapeutic approach for LSDs is the targeted gene therapy that uses genome-editing technologies, like

 doi:10.20944/preprints202511.1571.v1

CRISPR/Cas9. However, these strategies encounter several technical challenges and bioethical considerations, making it essential to study their effects *in vivo*, using animal models that can closely replicate LSD-specific phenotypes. Given the imminent need for robust *in vivo* models, we have, herein, generated transgenic *Drosophila* flies, via exploitation of the -combined- GAL4/UAS and RNAi gene-targeting system, to mechanistically illuminate LSD-associated pathologies, at the genetic level, during aging. This platform provides a dynamic, valuable and versatile tool to deeply investigate systemic pathologies and successfully explore novel therapies for LSD-affected cohorts.

2. Materials and Methods

2.1. Drosophila Melanogaster Strain Stocks and Culturing Conditions

The *Drosophila melanogaster* transgenic fly strains w[*]; P{w[+mC]=GAL4-elav.L}3 (RRID:BDSC_8760), y[1] sc[*] v[1] sev[21]; P{y[+t7.7] v[+t1.8]=TRiP.HMS01322}attP2 (RRID:BDSC_34334), y[1] v[1]; P{y[+t7.7] v[+t1.8]=TRiP.HMJ02101}attP40 (RRID:BDSC_53379), y[1] sc[*] v[1] sev[21]; P{y[+t7.7] v[+t1.8]=TRiP.HMC05804}attP2 (RRID:BDSC_64931), y[1] v[1]; P{y[+t7.7] v[+t1.8]=TRiP.HMC03475}attP40 (RRID:BDSC_51901), y[1] sc[*] v[1] sev[21]; P{y[+t7.7] v[+t1.8]=TRiP.HMS00562}attP2 (RRID:BDSC_33693), y[1] sc[*] v[1] sev[21]; P{y[+t7.7] v[+t1.8]=TRiP.HMS01646}attP40 (RRID:BDSC_37504), y[1] sc[*] v[1] sev[21]; P{y[+t7.7] v[+t1.8]=TRiP.HMS01681}attP40 (RRID:BDSC_38237), y[1] v[1]; P{y[+t7.7] v[+t1.8]=TRiP.HMJ30222}attP40 (RRID:BDSC_63655), y[1] sc[*] v[1] sev[21]; P{y[+t7.7] v[+t1.8]=TRiP.HMS05491}attP40 (RRID:BDSC_67025), y[1] sc[*] v[1] sev[21]; P{y[+t7.7] v[+t1.8]=TRiP.HMC06416}attP40 (RRID:BDSC_67312), y[1] sc[*] v[1] sev[21]; P{y[+t7.7] v[+t1.8]=TRiP.HMC04581}attP40 (RRID:BDSC_57199), y[1] sc[*] v[1] sev[21]; P{y[+t7.7] v[+t1.8]=TRiP.HMS01984}attP2 (RRID:BDSC_39064) and y[1] sc[*] v[1] sev[21]; P{y[+t7.7] v[+t1.8]=TRiP.HMS01893}attP40 (RRID:BDSC_38977) were obtained from Bloomington *Drosophila* Stock Center (NIH P40OD018537) (Indiana, USA). The *D. melanogaster* transgenic NP1-GAL4 fly strain was kindly provided by Dr. Eric H. Baehrecke [18] (Department of Cancer Biology, University of Massachusetts, Medical School, Worcester, MA, USA).

All fly stocks were maintained at 25 °C, in a relative humidity of 55-65%, under a 12-h light/dark photoperiod, and a laboratory standard *Drosophila* -nutrition- medium (6.4% rice flour, 5% tomato paste, 3.2% sugar, 0.8% yeast, 0.8% agar, 0.13% Tegosept, 0.4% ethanol and 0.4% propionic acid).

2.2. RNA Extraction and RT-qPCR

Isolation of total cellular RNA from RNAi-targeted fly heads was performed using the PureLink™ RNA Mini Kit (Invitrogen, Thermo Fisher Scientific, Waltham, MA, USA), according to manufacturer's instructions. Concentration and quality of the isolated RNA were determined using the NanoDrop One UV-Vis. spectrophotometer (Thermo Fisher Scientific, Waltham, MA, USA). First-strand cDNA was synthesized using the SuperScript™ IV First-Strand Synthesis System (Invitrogen, Thermo Fisher Scientific, Waltham, MA, USA), following manufacturer's protocol.

Relative expression of the, herein, studied genes was examined by Reverse Transcription (real-time) quantitative Polymerase Chain Reaction (RT-qPCR), using specific primers (Table S1), the Fast SYBR® Green Master Mix (Applied Biosystems, Thermo Fisher Scientific, Waltham, MA, USA) and the Applied Biosystems StepOne™ (real-time) qPCR System (Thermo Fisher Scientific, Waltham, MA, USA), as described by manufacturer's guidelines. As a suitable internal control, for normalization of gene expression values, the housekeeping gene *Actin 5C* was accordingly used. To ensure reproducibility, each assay was performed in technical triplicates, while three negative controls were also included in the analysis. Fold reductions in transcript levels were determined using the comparative $2^{-\Delta\Delta Ct}$ method [19], which calculates changes in gene expression as a relative fold difference between the gene(s) of interest and the reference gene. Results were presented as a percentage of the relative gene reduction in RNAi-targeted [specifically in neuronal (brain) tissues]

 doi:10.20944/preprints202511.1571.v1

flies, compared to control populations. Each experiment was performed three different times, using independent genetic crosses.

2.3. Longevity Measurement

To study viability, newly emerged (~24 h) female and male -transgenic- flies from each fly cross were collected and maintained in separate vials (~20-25 flies per vial). Flies were kept in a constant temperature and humidity chamber, throughout the experimental period, and periodically provided with fresh food every three days. Survival curves were generated by daily counting the deceased flies. For each viability experiment, the sample size was set to (at least) 100 flies per gender and genetic cross (to ensure statistical significance). All viability experiments were performed at the same time for control and RNAi-overexpressing strains. Each viability experiment was repeated (at least) three times, using independent genetic crosses.

2.4. Negative Geotaxis Assay

The locomotor performance of RNAi-targeted flies was quantified using the negative geotaxis (climbing) assay. Flies of both sexes were initially kept together, and, before the experimental procedure, they were anesthetized and divided into male and female populations (groups of ~20-25 flies, each). Each experimental group was, then, placed in an empty 100 ml cylinder, with a boundary line drawn at the 60 ml mark (10 cm height), and the flies were allowed for 1 min to acclimatize to the environment. To climb simultaneously, flies were gently tapped to the bottom of the cylinder. After time interval of 20 sec, the number of flies that reached or exceeded the 60 ml limit was counted. Five trials with 1 min-time interval were performed for each group. The same populations were tested at different ages, excluding flies that died or flew away. Control and RNAi-targeted fly groups were examined simultaneously. Total sample size for each fly cross and gender was set at (minimum) 100 flies. Three independent biological replicates were used for each fly group examined.

2.5. Structural Alignment

For the structural alignment of *Homo sapiens* (human) and *Drosophila* (fly) LSD-related proteins, AlphaFold-specific molecular models were obtained from the neural-network-based AlphaFold2 Protein Structure Database [20–22] and the generated protein models were structurally aligned with the PyMOL (v3.1) molecular graphics system [23]. The Root Mean Square Difference (RMSD) value of each alignment was used as an indicator for the reliability of structural alignment [24].

2.6. Statistical Analysis

Statistical analysis, and graphic presentation of the obtained results, were performed using the Statistical Package for Social Sciences (IBM SPSS v25.0 for Windows IBM Corp., New York, NY, USA). Data from the longevity experiments were analyzed with the Kaplan-Meier survival test, using the Log Rank, Breslow test and Tarone-Ware statistical packages. Climbing graphs were plotted as the mean pass rate per genotype/time-point with Sample Standard Deviation (± SSD) value. Statistically significant differences between the compared genotypes, at each time-point, were evaluated by the independent *t*-test analysis. Significance was accepted at: $p < 0.05$ (*), $p < 0.01$ (**) and $p < 0.001$ (***).

3. Results

3.1. From Humans to Flies: Identification of LSD-Related Gene Orthologs Using DIOPT

The first step for studying human disease genes in animal model organisms, such as *Drosophila*, is to recognize the putative orthologs that are being associated with the respective diseases. Ortholog genes facilitate functional genomics by allowing hypotheses concerning the functions of genes in one species to be deduced from their orthologs in another species. Therefore, to identify *Drosophila* orthologs of human LSD-related genes, the DRSC (*Drosophila* RNAi Screening Center) Integrative

 doi:10.20944/preprints202511.1571.v1

Ortholog Prediction Tool (DIOPT) [25] was suitably engaged. DIOPT integrates the results of multiple ortholog-mapping tools based on different algorithms and calculates a simple score reflecting the number of tools that support a given ortholog gene-pair relationship. In version 9, the maximum score for fly-human ortholog relationship is 19, in an 1-19 scale. Based on this score, DIOPT also provides ortholog ranks, being categorized as high, moderate and low, which reflect the confidence level in predicted "orthology" relationships between genes of different species [25,26]. In Table 1, we present a DIOPT-derived extensive list, corresponding to nearly all human LSD-related genes, along with their putative orthologs in *Drosophila*. In addition, we provide the DIOPT ranking and the associated RNAi strains available from the Bloomington (BDSC) and Vienna (VDRC) [27] *Drosophila* Stock/Resource Centers, thus offering a useful resource for designing genetic studies on evolutionary conserved disease genes.

Following ortholog prediction, we focused on screening LSDs not previously studied in *Drosophila* or examined using alternative genetic tools. Our overall objective is to identify novel genotype–phenotype associations between humans and *Drosophila*, to advance our understanding of the molecular mechanisms underlying LSDs. In an effort to, *in vivo*, investigate the importance of LSD-related genes at the organ(ism) level, we, next, proceeded to the targeted gene knockdown of their *Drosophila* orthologs, through employment of the GAL4/UAS genetic system in combination with the RNAi technology [27,28]. Gene silencing was carried out in a tissue-specific manner, along the brain-midgut axis, and the phenotypic assays engaged to quantify gene-function aberrations were life expectancy and climbing capacity. Locomotor impairment was specifically evaluated in *Drosophila* disease models that exhibited the most pronounced reductions in lifespan along the brain-midgut axis, as these models could most effectively recapitulate key pathological features and were, therefore, deemed the most robust representative systems for the respective human disorders. Negative geotaxis (climbing activity) is a commonly used method for evaluating neuronal dysfunction in flies that results from neuron-specific silencing of selected genes/proteins [29]. For all LSDs, herein examined, the predicted *Drosophila* orthologs being selected for further investigation were characterized by high or moderate DIOPT rankings (Table 1).

Table 1. *Drosophila* orthologs of human Lysosomal Storage Disorder (LSD)–associated genes identified via DIOPT.

Lysosomal Storage Disorders (*LSDs*)	**Human Gene**	**Protein Name**	***Drosophila* Ortholog**	**Homology (*Rank*) (*DIOPT Score*)**	**RNAi Strain**
1. Autosomal recessive spastic paraplegia type 48 (SPG48)	*AP5Z1*	Adaptor-related protein complex 5 subunit zeta 1	*Lpin* / *CG8709*	Low (1)	63614[1] 77170[1]
2. Disorders of lysosomal amino acid transport					
A. Cystinosis	*CTNS*	Cystinosin, Lysosomal Cystine transporter	*Ctns* / *CG17119*	High (16)	40823[1]
B. Free sialic acid storage disease (free SASD)					
a) Salla disease (SD)	*SLC17A5*	Sialin, Solute carrier family 17 member 5	*VGlut2* / *MFS9* / *CG4288*	High (10)	29305[1]
b) Intermediate severity Salla disease					v104145[2]

 doi:10.20944/preprints202511.1571.v1

c) Infatile free sialic acid storage disease (ISSD)					
3. Disorders of sialic acid metabolism					
Sialuria	*GNE*	Glucosamine (UDP-N-acetyl)-2-epimerase / N-Acetyl-mannosamine kinase	-	-	-
4. Glycoproteinoses					
A. Mucolipidoses (ML)					
a) ML type II α/β: Inclusion (I)-cell disease	*GNPTAB*	N-Acetyl-glucosamine-1-phosphotransferase subunits α/β	*Gnptab / CG8027*	High (15)	v109400[2]
b) ML type III: Pseudo-Hurler polydystrophy:					
type III α/β	*GNPTG*	N-Acetyl-glucosamine-1-phosphotransferase subunit γ	*GCS2beta / CG6453*	Moderate (3)	35008[1]
type III γ			*CG7685*	Low (2)	62254[1]
c) ML type IV: Sialolipidosis	*MCOLN1*	Mucolipin 1, Mucolipin transient receptor potencial (TRP) cation channel 1	*CG42638*	Moderate (14)	44098[1]
			Trpml / CG8743	Moderate (14)	31294[1]
					31673[1]
					v108088[2]
					v45989[2]
B. Oligosaccharidoses					
a) α-Mannosidosis	*MAN2B1*	Lysosomal α-Mannosidase, Mannosidase alpha class 2B member 1	*LManII / CG6206*	High (16)	53294[1]
			LManI / CG5322	Moderate (14)	44473[1]
			LManV / CG9466	Moderate (14)	v104300[2]
					v13040[2]
			LManIV / CG9465	Moderate (14)	66992[1]
			LManIII / CG9463	Moderate (13)	v15589[2]
					v48063[2]
			LManVI / CG9468	Moderate (12)	61216[1]
			alpha-Man-IIa / CG18802	Low (3)	v5838[2]

 doi:10.20944/preprints202511.1571.v1

			alpha-Man-IIb / CG4606	Low (2)	v108 043[2]
					v426 52[2]
b) β-Mannosidosis	*MANBA*	β-Mannosidase	*beta-Man / CG12582*	High (14)	5327 2[1]
c) Fucosidosis	*FUCA 1*	α-L-Fucosidase 1	*Fuca / CG6128*	High (13)	-
d) Aspartyglucosaminuria (AGU)	*AGA*	Aspartylglucosaminidase	*CG1827*	High (14)	6514 1[1]
			CG10474	High (14)	5144 4[1]
			CG4372	Moderate (8)	v364 31[2]
			CG7860	Low (2)	v108 281[2]
					v343 94[2]
			Tasp1 / CG5241	Low (2)	6490 7[1]
e) α-N-Acetyl-galactosaminidase deficiency (NAGA deficiency): Schindler disease:					
type I: Infantile onset Neuroaxonal dystrophy	*NAGA*	α-N-Acetyl-galactosaminidase	*CG5731*	High (16)	6702 5[1]
type II: Kanzaki disease			*CG7997*	Moderate (15)	6365 5[1]
type III: Intermediate severity					5778 1[1]
f) Galactosialidosis: Goldberg syndrome	*CTSA*	Protective protein Cathepsin A, and a secondary deficiency in β-Galactosidase and Neuraminidase-1	*CG4572*	Moderate (4)	3433 7[1]
			CG32483	Low (2)	v106 263[2]
					v229 76[2]
			hiro / CG3344	Low (2)	v110 402[2]
					v152 13[2]
			CG31821	Low (2)	v106 059[2]
					v154 96[2]
			CG31823	Low (2)	6694 1[1]
					6702 7[1]
g) Sialidosis:					

 doi:10.20944/preprints202511.1571.v1

type I (ST-1): Cherry-red spot-myoclonus syndrome	*NEU1*	Neuraminidase-1, Lysosomal Sialidase	-	-	-
type II (ST-2): Mucolipidosis I					
5. Lysosomal acid phosphatase deficiency					
6. Glycogen storage disease(s) [GSD(s)]					
GSD type II (due to acid maltase deficiency): Pompe disease	*GAA*	Lysosomal α-Glucosidase, Acid maltase	*GCS2alpha / CG14476*	Moderate (5)	34334[1]
			tobi / CG11909	Low (3)	53379[1]
			CG33080	Low (2)	42554[1]
GSD due to LAMP-2 deficiency: Danon disease	*LAMP 2*	Lysosomal-associated membrane protein 2	*Lamp1 / CG3305*	Moderate (8)	38335[1]
					38254[1]
			CG32225	Low (3)	v102345[2]
					v5383[2]
7. Mucopolysaccharidoses (MPSs)					
MPS I:					
Hurler syndrome (MPSIH)	*IDUA*	α-L-Iduronidase	*Idua / CG6201*	High (14)	64931[1]
Hurler-Scheie syndrome (MPSIH/S)					
Scheie syndrome (MPSIS)					
MPS II: Hunter syndrome					
type A (MPSIIA), severe form	*IDS*	Iduronate 2-sulfatase	*Ids / CG12014*	High (18)	51901[1]
type B (MPSIIB), attenuated form					63004[1]
MPS III: Sanfilippo syndrome:					
type A (MPSIIIA)	*SGSH*	N-Sulfoglucosamine sulfohydrolase	*Sgsh / CG14291*	High (16)	v107384[2]
					v16897[2]
type B (MPSIIIB)	*NAGLU*	N-Acetyl-α-glucosaminidase	*Naglu / CG13397*	High (17)	51808[1]
type C (MPSIIIC)	*HGSNAT*	Heparan-α-glucosaminide N-acetyltransferase	*Hgsnat / CG6903*	High (15)	33423[1]
type D (MPSIIID)	*GNS*	N-Acetylglucosamine-6-sulfatase	*Gns / CG18278*	High (15)	285201[1]
					518781[1]
					v109944[2]

 doi:10.20944/preprints202511.1571.v1

					v22936[2]
MPS IV: Morquio syndrome:					
type A (MPSIVA)	*GALNS*	N-Acetylgalactosamine-6-sulfatase	*CG7408*	Moderate (3)	65359[1]
			Gns / CG18278	Moderate (3)	28520[1]
					51878[1]
			CG7402	Moderate (3)	v103947[2]
					v37302[2]
			CG32191	Moderate (3)	v101578[2]
					v14294[2]
type B (MPSIVB)	*GLB1*	β-Galactosidase 1	*Ect3 / CG3132*	Moderate (15)	62217[1]
			Gal / CG9092	Moderate (14)	42922[1]
					50680[1]
MPS VI: Maroteaux-Lamy syndrome	*ARSB*	Arylsulfatase B	*CG7402*	High (13)	v103947[2]
					v37302[2]
MPS VII: Sly disease	*GUSB*	β-Glucuronidase	*CG15117*	High (17)	33693[1]
			beta-Glu / CG2135	Moderate (15)	62236[1]
			beta-Man / CG12582	Low (2)	53272[1]
MPS IX: Hyaluronidase deficiency	*HYAL1*	Hyaluronidase 1	-	-	-
8. Neuronal ceroid lipofuscinoses (NCL): Batten disease					
CLN1: Haltia-Santavuori disease / Hagberg-Santavuori disease / Santavuori disease (INCL)	*PPT1*	Palmitoyl-protein thioesterase 1	*Ppt1 / CG12108*	High (14)	55331[1]
					62291[1]
					25952[1]
			Ppt2 / CG4851	Low (3)	28362[1]
					v106819[2]
					v1459[2]

 doi:10.20944/preprints202511.1571.v1

CLN2: Jansky-Bielschowsky disease (LINCL)	*TPP1*	Tripeptidyl peptidase 1	-	-	-
CLN3: Batten-Spielmeyer-Sjogren disease (JNCL)	*CLN3*	Battenin, Endosomal transmembrane protein	*Cln3 / CG5582*	High (14)	35734[1]
CLN4: Parry disease / Kufs disease type A and B (ANCL)	*DNAJC5*	Cysteine string protein, DnaJ Heat shock protein family (Hsp40) member C5	*Csp / CG6395*	High (14)	33645[1]
					31290[1]
					31669[1]
			CG7130	Low (2)	57854[1]
			CG7133	Low (2)	60459[1]
					42820[1]
			l(3)80Fg / CG40178	Low (2)	44578[1]
CLN5: Finnish variant	*CLN5*	Ceroid-lipofuscinosis neuronal protein 5	-	-	-
CLN6: Lake-Cavanagh or Indian variant	*CLN6*	Transmembrane ER protein	-	-	-
CLN7: Turkish variant	*MFSD8*	Major-facilitator superfamily domain containing 8	*Cln7 / CG8596*	High (16)	61960[1]
					55664[1]
			rtet / CG5760	Low (2)	v110473[2]
					v44002[2]
CLN8: Northern epilepsy / Epilepsy mental retardation	*CLN8*	Protein CLN8, Transmembrane ER and ERGIC protein	*CG17841*	Moderate (3)	34948[1]
CLN9	N/A	N/A			
CLN10: Congenital NCL	*CTSD*	Cathepsin D, Lysosomal Aspartyl peptidase / protease	*cathD / CG1548*	High (16)	28978[1]
					53882[1]
					55178[1]
CLN11	*GRN*	Granulin (precursor)	*CG15011*	Low (1)	58284[1]
					31589[1]
			NimC2 / CG18146	Low (1)	25960[1]
					v3120[2]
					v36261[2]
CLN12: Kufor-Raked syndrome /	*ATP13A2*	Cation-transporting ATPase 13A2, PARK9	*anne / CG32000*	Moderate	44005[1]

 doi:10.20944/preprints202511.1571.v1

PARK9 / Juvenile parkinsonism-NCL				(13)	30499[1]
			CG6230	Low (3)	77371[1]
			SPoCk / CG32451	Low (2)	44040[1]
					28352[1]
CLN13	*CTSF*	Cathepsin F	*CtsF / CG12163*	High (14)	33955[1]
CLN14: Progressive myoclonic epilepsy type 3	*KCTD7*	Potassium channel tetramerization domain containing 7	*Ktl / CG10830*	Moderate (2)	57171[1]
					25848[1]
			CG14647	Moderate (2)	60064[1]
					27032[1]
			twz / CG10440	Moderate (2)	57397[1]
					25846[1]
9. Pycnodysostosis: Toulouse-Lautrec syndrome – Osteopetrosis acro-osteolytica	*CTSK*	Cathepsin K	*CtsL1 / CG6692*	Moderate (8)	41939[1]
					32932[1]
10. Sphingolipidoses					
A. Acid sphingomyelinase deficiency (ASMD)					
Niemann-Pick disease types A and B	*SMPD1*	Sphingomyelin phosphodiesterase	*Asm / CG3376*	High (17)	36760[1]
			CG15533	Moderate (8)	36761[1]
			CG15534	Moderate (8)	36762[1]
			CG32052	Moderate (6)	36763[1]
B. Autosomal recessive cerebellar ataxia with late-onset spasticity (due to GBA2 deficiency)	*GBA2*	β-Glucosylceramidase 2	*CG33090*	High (18)	36688[1]
C. Encephalopathy due to prosaposin deficiency - Combined PSAP deficiency (PSAPD)	*PSAP*	Prosaposin	*Sap-r / CG12070*	High (14)	v51129[2]
					v51130[2]
D. Fabry disease – Angiokeratoma corporis diffusum	*GLA*	α-Galactosidase A	*CG7997*	Moderate (14)	63655[1]
					57781[1]

 doi:10.20944/preprints202511.1571.v1

			CG5731	Moderate (13)	67025[1]
E. Farber lipogranulomatosis	*ASAH1*	Acid Ceramidase	-	-	-
F. Gangliosidoses					
a) GM1 gangliosidosis: Landing disease:					
type I (infantile): Norman-Landing disease	*GLB1*	β-Galactosidase	*Ect3 / CG3132*	Moderate (15)	62217[1]
type II (juvenile - late infantile)			*Gal / CG9092*	Moderate (14)	50680[1]
type III (adult)					42922[1]
b) GM2 gangliosidosis:					
Tay-Sachs disease (B variant)	*HEXA*	β-Hexosaminidase subunit α	*Hexo1 / CG1318*	Moderate (13)	67312[1]
			Hexo2 / CG1787	Moderate (12)	57199[1]
			fdl / CG8824	Moderate (11)	52987[1]
					28298[1]
Sandhoff disease (0 variant)	*HEXB*	β-Hexosaminidase subunit β	*Hexo1 / CG1318*	High (14)	67312[1]
			Hexo2 / CG1787	Moderate (12)	57199[1]
			fdl / CG8824	Moderate (12)	52987[1]
					28298[1]
c) GM2 activator deficiency (AB variant)	*GM2A*	GM2 Ganglioside activator	-	-	-
G. Gaucher disease (GD)					
GD type 1	*GBA1*	β-Glucocerebrosidase 1 / β-Glucosidase 1	*Gba1a / CG31148*	High (15)	38379[1]
GD type 2					39064[1]
GD type 3			*Gba1b / CG31414*	High (15)	38970[1]
Fetal / Perinatal lethal Gaucher disease					38977[1]
Atypical Gaucher disease due to Saposin C deficiency	*PSAP*	Prosaposin	*Sap-r / CG12070*	High (14)	v51129[2]
					v51130[2]
Gaucher-like disease / Gaucher disease-	*GBA1*	β-Glucosylceramidase 1	*Gba1a / CG31148*	High (15)	38379[1]

 doi:10.20944/preprints202511.1571.v1

ophthalmoplegia-cardiovascular calcification syndrome / Gaucher disease type 3C					39064[1]
			Gba1b / *CG31414*	High (15)	38970[1]
					38977[1]
H. Globoid cell leukodystrophy – Krabbe disease	*GALC*	Galactosylceramidase	-	-	-
I. Lipid storage disease					
a) Lysosomal acid lipase deficiency					
Cholesterol ester storage disease	*LIPA*	Lipase A lysosomal acid type, Cholesterol ester hydrolase	*Lip3* / *CG8823*	High (15)	65025[1]
Wolman disease					
b) Niemann-Pick disease type C:					
type C1	*NPC1*	NPC Intracellular cholesterol transporter 1	*Npc1a* / *CG5722*	High (16)	37504[1]
			Npc1b / *CG12092*	Moderate (11)	38296[1]
			SCAP / *CG33131*	Low (2)	31566[1]
type C2	*NPC2*	NPC Intracellular cholesterol transporter 2	*Npc2a* / *CG7291*	High (16)	38237[1]
			Npc2b / *CG3153*	Moderate (7)	38238[1]
					42914[1]
			Npc2d / *CG12813*	Moderate (6)	v31095[2]
			Npc2c / *CG3934*	Moderate (6)	61315[1]
			Npc2e / *CG31410*	Moderate (6)	67956[1]
			Npc2f / *CG6164*	Moderate (4)	v102172[2]
					v12915[2]
			Npc2h / *CG11315*	Moderate (3)	67803[1]
			Npc2g / *CG11314*	Moderate (3)	63030[1]
J. Metachromatic leukodystrophy (MLD)	*ASRA PSAP*	Arylsulfatase A Prosaposin			

 doi:10.20944/preprints202511.1571.v1

K. Multiple Sulfatase deficiency (MSD) / Mucosulfatidosis	*SUMF 1*	Sulfatase modifying factor 1, Formylglycine-generating enzyme	*CG7049*	High (14)	51896[1]
Action myoclonus-renal failure syndrome / Myoclonus-nephropathy syndrome / Progressive myoclonic epilepsy type 4	*SCARB2*	Scavenger receptor class B member 2, Lysosomal integral membrane protein II	*emp* / *CG2727*	High (15)	40947[1]

[1] Bloomington *Drosophila* Stock Center; [2] Vienna *Drosophila* Resource Center; N/A: Not Applicable.

3.2. Structural Conservation of LSD-Associated Proteins Between Homo Sapiens and Drosophila Melanogaster

Three-dimensional structural alignment, via PyMOL [30] engagement, is a valuable tool for revealing structural conservation between ortholog proteins with high sequence similarity and for gaining insights into their structural characteristics. Initially, all selected LSD-related structures of human and *Drosophila* proteins were retrieved from the neural network-based protein-structure prediction tool AlphaFold2 [20–22]. Next, PyMOL alignment was employed, with sequence alignment being followed by structural superposition and subsequent minimization of the Root Mean Square Deviation (RMSD) between the aligned residues through the execution of refinement cycles to reject structural outliers identified during alignment. RMSD value between corresponding atoms of two protein chains is the most common estimator of structural similarity, with RMSD below 3 Å typically indicating close homology [24]. Interestingly, protein comparisons of all *Drosophila* orthologs derived from DIOPT, carrying high or moderate homologies to their human LSD-related counterparts, yielded low RMSD values, ranging from 0.454 to 1.376 Å, with their majority being measured below 1 Å (Figures S1-S8), thus indicating minor structural variation. Only the comparison of protein structures being produced from the human gene *GAA* (implicated in Pompe disease) and its *Drosophila* ortholog *Tobi* (Figure S5), which shows low homology in DIOPT, resulted in a high RMSD value of 3.291 Å, strongly suggesting a comparatively larger disparity between the human and fly respective gene products. For all the alignments, herein examined, each *Drosophila* protein structure was aligned to (superimposed with) the human reference, respective, structure. The high degree of structural similarity observed between the aligned (superimposed) ortholog proteins not only reflects their evolutionarily conserved architecture, but also indicates conserved functional properties and roles, thereby strongly supporting the validity of using *Drosophila* as a powerful, versatile and multifaceted -animal- model system for *in vivo* investigating human LSD-linked pathologies.

3.3. Modeling of Sphingolipidoses in Drosophila

3.3.1. Gaucher Disease

Sphingolipidoses constitute an essential group of LSDs that are being characterized by the accumulation of sphingolipids [10]. Among them, Gaucher disease is the most common one [2] and is distinguished in three different subtypes, all caused by mutations in the *GBA1* gene [4]. A DIOPT analysis to identify *Drosophila melanogaster* orthologs revealed two candidate genes, *Gba1a* and *Gba1b*, both exhibiting high homology scores (Table 1), and encoding protein products with strong structural similarities to their human counterparts (Figures 1A and 2A, for Gba1a and Gba1b, respectively). Therefore, we, next, proceeded to the tissue-specific, RNAi-mediated, downregulation of both *Drosophila* orthologs, along the brain-midgut axis. To validate the efficiency of gene silencing, and thus the reliability of our genetic models, we quantified *Gba1a* and *Gba1b* gene expression levels following neuronal-specific knockdown. The analysis revealed a significant reduction in mRNA expression of ~46% for *Gba1a* (Figure 1B) and ~53% for *Gba1b* (Figure 2B), relative to control fly brains.

 doi:10.20944/preprints202511.1571.v1

RNAi-mediated downregulation of *Gba1a* or *Gba1b* gene, specifically in the nervous system (brain), caused a severe decrease in male fly-life expectancy, with a median survival reduction of ~31 and ~34 days, respectively, compared to control male flies (Figures 1C and 2C). Although female flies also exhibited reduced median survival, in response to neuronal-specific (brain) knockdown of either gene, their pathogenic effects were notably less pronounced as compared to male ones (Figures 1C and 2C). Regarding midgut-specific knockdown models, only male flies demonstrated significantly decreased survival rates (Figures 1D and 2D), with the obtained pathology being comparatively more severe in the *Gba1b*-specific, RNAi-targeted, flies.

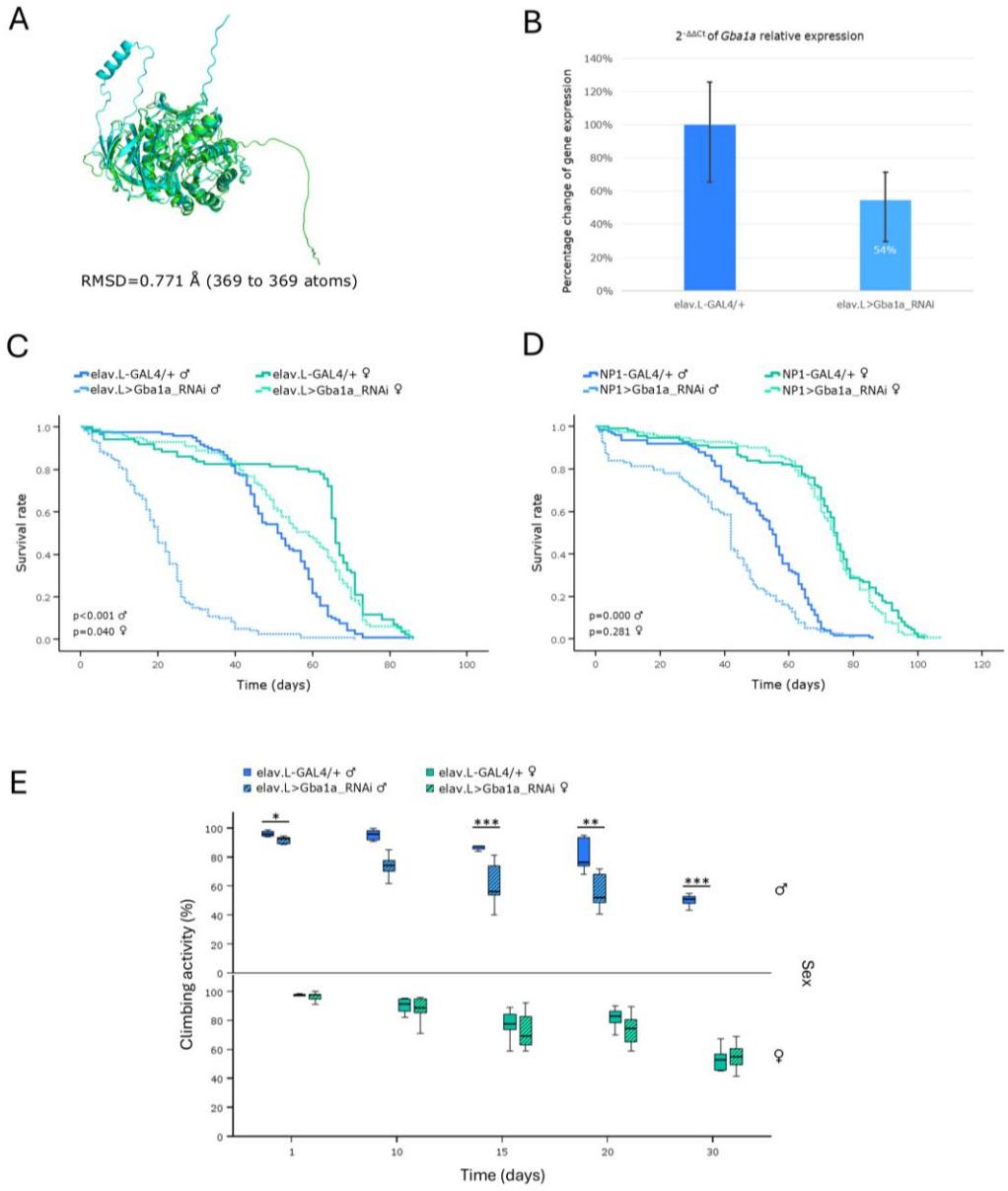

Figure 1. *In vivo* genetic modeling of Gaucher disease in *Drosophila*, via *Gba1a* ortholog-gene targeting, specifically in the brain-midgut axis. (A) Structural alignment of AlphaFold-predicted protein structures being encoded by the human *GBA1* gene (light green) and its *Drosophila* ortholog *Gba1a* (light cyan). The human protein structure was aligned to the *Drosophila* respective structure, using the PyMOL molecular graphics system. (B) Relative expression analysis of the *Gba1a* gene in fly neuronal (brain) tissues following its (*Gba1a*) RNAi-mediated knockdown (elav.L>Gba1a_RNAi), compared to control flies (elav.L-GAL4/+), as determined by real-time qPCR technology. (C) Lifespan profiling of male and female flies following *Gba1a* gene knockdown, specifically in the nervous system (brain). (D) Survival curves of male and female flies being subjected to *Gba1a* gene downregulation, specifically in midgut tissues (NP1>Gba1a_RNAi). (E) Climbing performance (negative

 doi:10.20944/preprints202511.1571.v1

geotaxis assay) of male and female flies with neuronal-specific (brain) *Gba1a* gene silencing, during aging (0-30 days, post-eclosion). *$p < 0.05$, **$p < 0.01$ and ***$p < 0.001$.

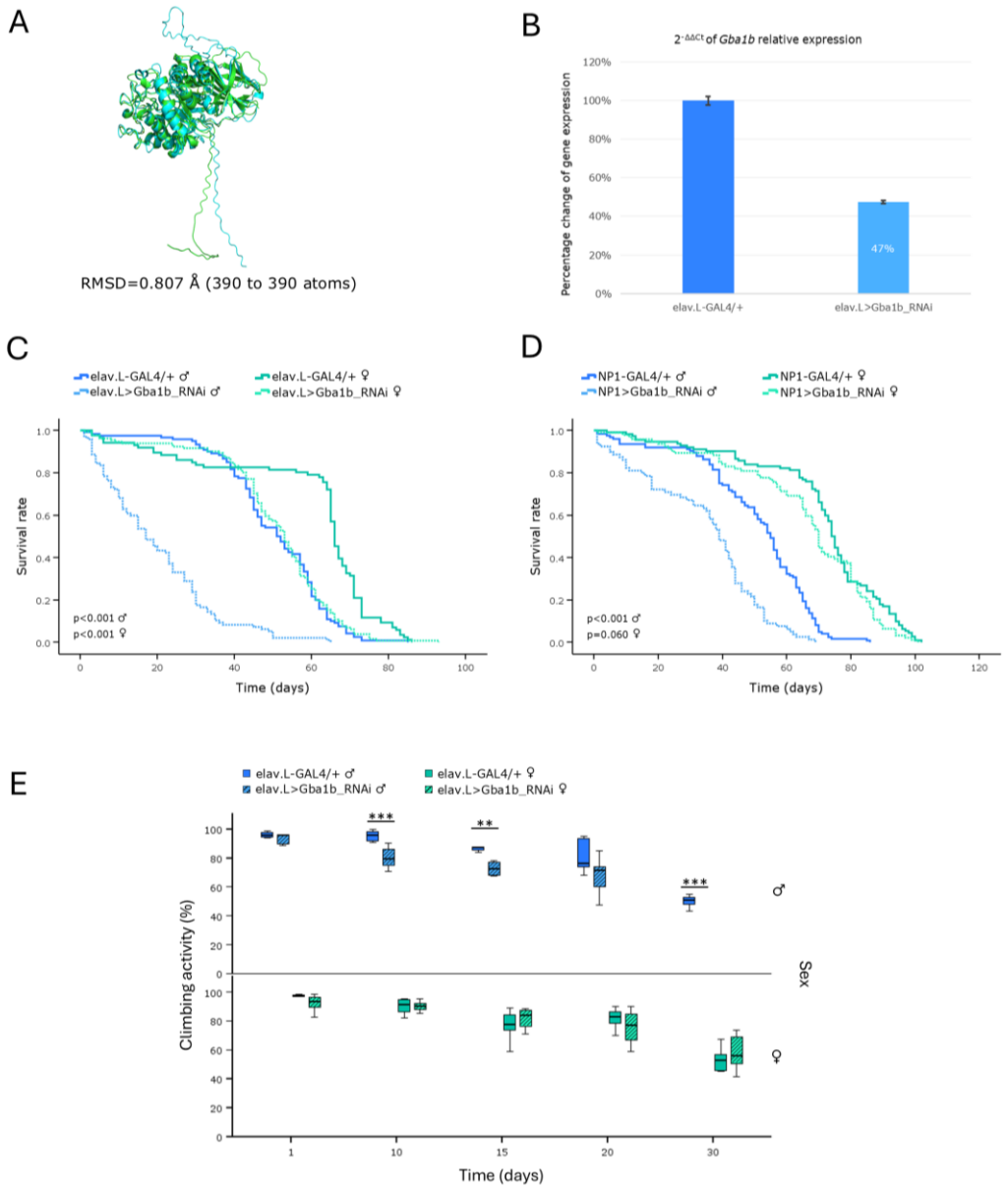

Figure 2. Genetic modeling of Gaucher disease in *Drosophila* brain-midgut axis, via *Gba1b* ortholog-gene targeting, *in vivo*. (**A**) Structural alignment of AlphaFold-derived protein structures being encoded by the human *GBA1* gene (light green) and its *Drosophila* ortholog *Gba1b* gene (light cyan), with the human reference protein being aligned to the *Drosophila* one through employment of the PyMOL molecular graphics system. (**B**) Relative expression levels of the *Gba1b* gene in neuronal (brain) tissues of RNAi-targeted flies (elav.L>Gba1b_RNAi), compared to control flies (elav.L-GAL4/+), having been measured by real-time qPCR. (**C**) Survival curves of male and female flies, following *Gba1b* gene knockdown, specifically in the nervous system (brain). (**D**) Lifespan profiles of male and female flies after *Gba1b* gene silencing, specifically in midgut tissues (NP1>Gba1b_RNAi). (**E**) Climbing-activity (negative-geotaxis) patterns of male and female transgenic flies carrying downregulated Gba1b protein contents, specifically in the nervous system (brain), during aging (0-30 days, post-eclosion). **$p < 0.01$ and ***$p < 0.001$.

Furthermore, compared to control flies, adult males with either *Gba1a* or *Gba1b* gene-knockdown profile, specifically in the nervous system (brain), displayed progressive, age-dependent, locomotor defects (Figures 1E and 2E), which comparatively proved more detrimental after 10 days of age, post-eclosion. Of note, due to the high mortality levels of male *Gba1a*- and *Gba1b*-targeted (via RNAi) flies,

 doi:10.20944/preprints202511.1571.v1

specifically in neuronal tissues (brain), we were unable to collect -statistically- sufficient numbers of fly individuals, for reliably conducting climbing experiments at the 30th day of age, post-eclosion. In contrast, female flies with neuronal-specific (brain) knockdown of either gene retained relatively normal climbing performance compared to their control counterparts (Figures 1E and 2E for *Gba1a*-RNAi and *Gba1b*-RNAi flies, respectively).

Taken together, the RNAi-mediated knockdown of either *Gba1a* or *Gba1b Drosophila* orthologs of human *GBA1* gene proved able to strikingly recapitulate key pathogenic features of Gaucher disease, strongly supporting the *in vivo* power and value of the fly brain-midgut axis, for reliably modeling and illuminating disease mechanisms, and promptly discovering therapeutic regimens.

3.3.2. Fabry Disease

Fabry disease is an X-linked monogenic disorder and it has been reported as the second most common LSD [10]. In humans, the disease is caused by mutations in the *GLA* gene, which encodes the Lysosomal α-Galactosidase A, an enzyme responsible for the hydrolysis of globotriaosylceramide. In *Drosophila*, two orthologs (*CG7997* and *CG5731*) of the human *GLA* gene have been identified. Although both genes receive moderate rankings and modest DIOPT scores (Table 1), the structural comparisons of their cognate protein products (CG7997 and CG5731) to the human counterpart (GLA) reveal very low RMSD values (below 0.5 Å; Figures 3A and 4A), thus indicating the high degree of structural conservation (during species evolution). RNAi-mediated, neuronal (brain)-specific, knockdown of the *CG7997* and *CG5731* genes led to a decrease in mRNA expression of ~8% and ~61%, respectively, compared to control flies (Figures 3B and 4B). As expected from the low knockdown efficiency of *CG7997*, the lifespan of flies being subjected to RNAi-mediated silencing of this gene, along the brain-midgut axis, did not significantly differ from that of control fly population (Figures 3C and D). In contrast, knockdown of *CG5731*, in either the nervous system (brain) or midgut tissues, resulted in flies with significantly shortened life expectancy (Figures 4C and D). Interestingly, female flies were more severely affected, exhibiting a median lifespan reduction of~28 days following neuronal (brain)-specific knockdown and of ~40 days after midgut-specific silencing of the *CG5731* gene (Figures 4C and D).

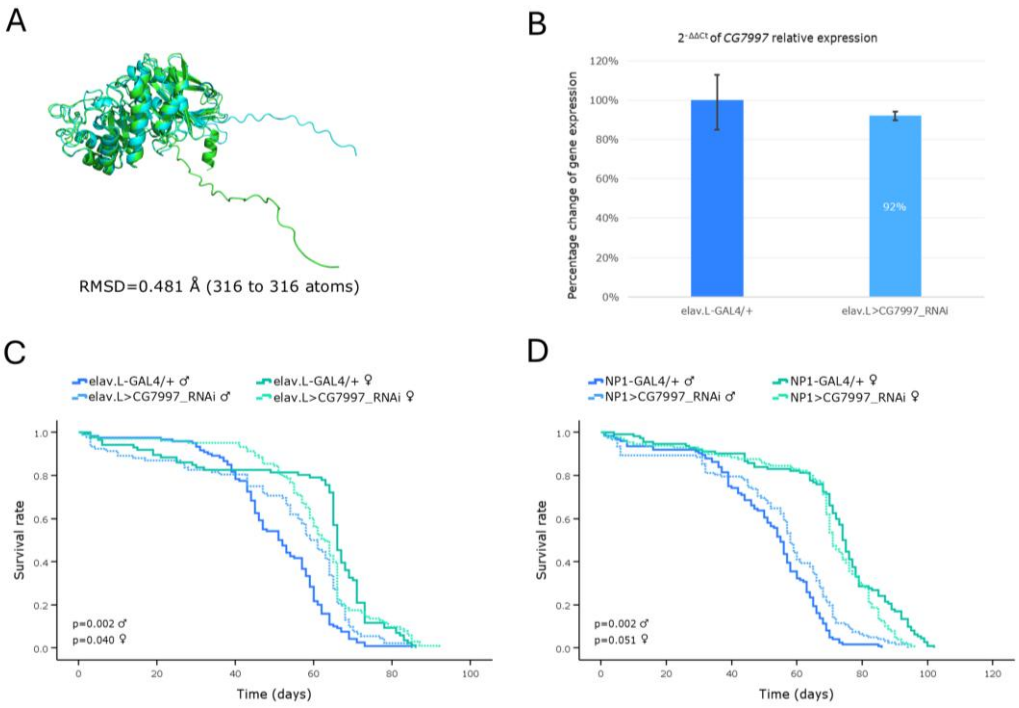

Figure 3. Genetic modeling of Fabry disease in *Drosophila* brain-midgut axis, through targeting the *CG7997* ortholog gene, *in vivo*. (A) PyMOL-mediated structural alignment of the AlphaFold-generated protein structure

 doi:10.20944/preprints202511.1571.v1

of the human *GLA* gene (light green) aligned to its *Drosophila* counterpart that is being encoded by the *CG7997* ortholog (light cyan). (B) Relative expression levels of the *CG7997* gene in neuronal (brain) tissues of RNAi-targeted flies (elav.L>CG7997_RNAi), compared to control (elav.L-GAL4/+) population, through engagement of the real-time qPCR technology. (C) Survival curves of flies, for both sexes, following *CG7997* gene knockdown, specifically in the nervous system (brain). (D) Lifespan profiles of male and female flies, after *CG7997* gene silencing, specifically in midgut tissues (NP1>CG7997_RNAi).

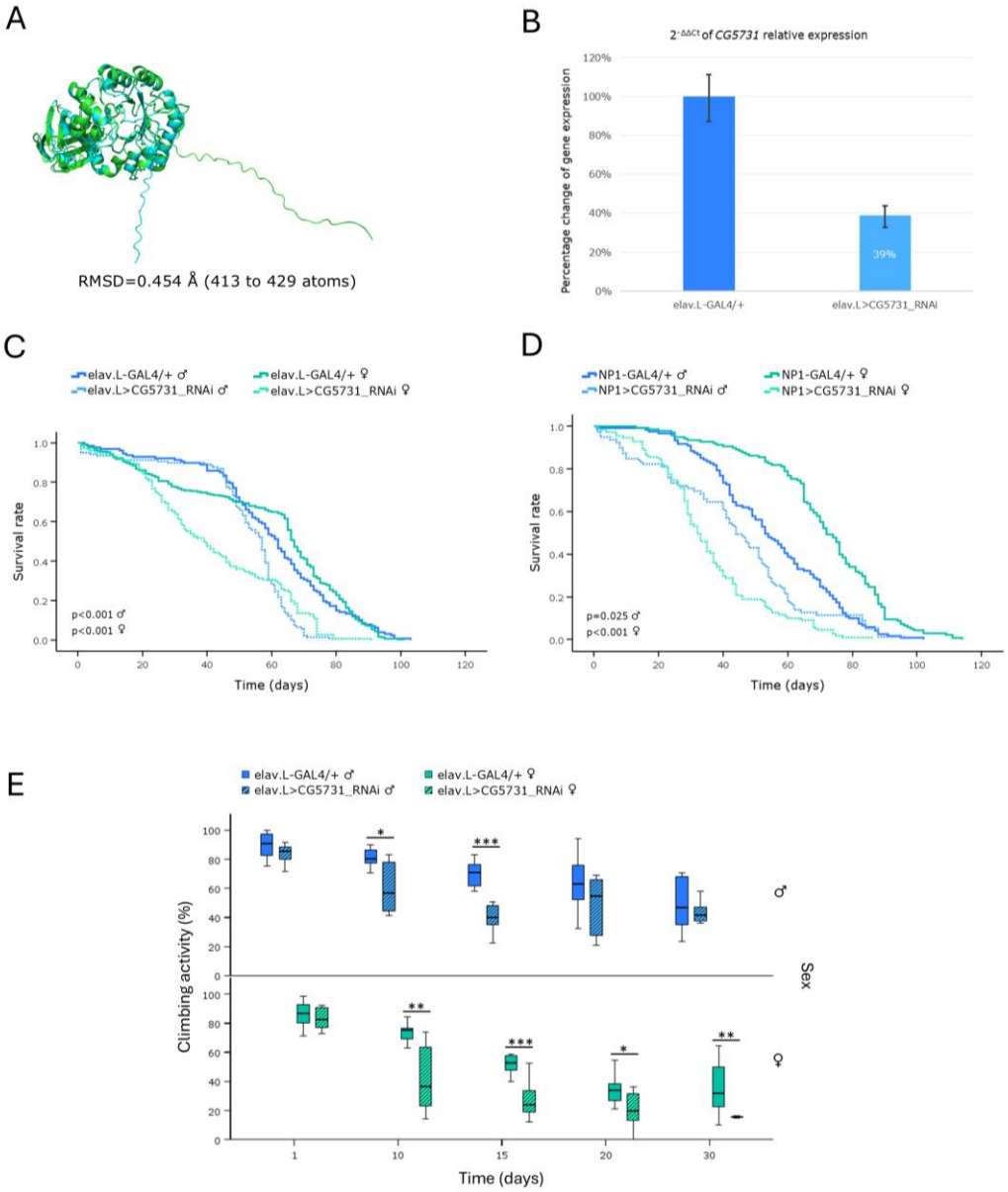

Figure 4. *In vivo* genetic modeling of Fabry disease in *Drosophila*, via RNAi-mediated targeting of *CG5731* ortholog gene, in the brain-midgut axis, during aging. (A) Structural alignment of AlphaFold-derived protein structures of human *GLA* (light green) and its *Drosophila* ortholog *CG5731* (light cyan), having been generated and visualized using the PyMOL molecular graphics system. The human reference sequence (GLA) is aligned to the *Drosophila* protein (CG5731). (B) Quantitative analysis of *CG5731* mRNA levels in neuronal (brain) tissues of $CG5731^{RNAi}$-expressing flies (elav.L>CG5731_RNAi), relatively to control (elav.L-GAL4/+), using real-time qPCR technology. (C) Survival curves of male and female flies, following nervous system (brain)-specific silencing of the *CG5731* gene. (D) Viability profiles of flies being characterized by targeted *CG5731* knockdown, specifically in midgut tissues (NP1>CG5731_RNAi) (compared to control). (E) Negative-geotaxis (climbing-activity) assay, during aging (0-30 days, post-eclosion), demonstrating progressive locomotor decline in flies

 doi:10.20944/preprints202511.1571.v1

with neuronal (brain)-specific *CG5731* downregulation, compared to control fly population. *$p < 0.05$, **$p < 0.01$ and ***$p < 0.001$.

Furthermore, flies of both sexes presented locomotor deficiencies, as early as day 10 post-eclosion, after neuronal (brain)-specific knockdown of the *CG5731* gene, as demonstrated by the negative-geotaxis (climbing-activity) assay (Figure 4E). The observation that female flies, compared to male populations, are more severely affected by the *CG5731* downregulation, may be mechanistically associated with differences in sex-dependent metabolic demand and hormonal regulation, and/or sexually dimorphic tissue-specific gene expression patterns.

3.3.3. Niemann-Pick Disease

Niemann-Pick disease types C1 and C2 are caused by mutations in the *NPC1* and *NPC2* gene loci, leading to impaired intracellular cholesterol trafficking, and subsequent accumulation of cholesterol and sphingolipids in lysosomes [4,12]. In *Drosophila*, the DIOPT tool recognized *Npc1a* and *Npc2a*, as high confidence orthologs of human *NPC1* and *NPC2* genes, respectively (Table 1). Furthermore, structural alignment analysis yielded RMSD values below 1 Å, for both the *NPC1-Npc1a* and *NPC2-Npc2a* protein product comparisons, thus indicating a high degree of structural similarity between the human and *Drosophila* proteins (during species evolution) (Figures 5A and 6A). Neuronal (brain)-specific downregulation of *Npc1a* and *Npc2a* genes resulted in ~14% and ~58% reductions in mRNA expression levels (Figures 5B and 6B), respectively. Interestingly, albeit the moderate knockdown efficiency in the *Npc1a*-targeted flies, both male *Drosophila* Niemann-Pick models exhibited a significant decrease in lifespan, along the brain-midgut axis, with their median life expectancy being reduced by ~29 (Figure 5C; *Npc1α* targeting) and ~26 (Figure 6C; *Npc2α* targeting) days, following neuronal (brain)-specific downregulation, and ~20 (Figure 5D; *Npc1α* targeting) and ~17 (Figure 6D; *Npc2α* targeting) days, after midgut-specific targeting of the fly ortholog -respective- genes.

In contrast, female flies presented only a modest reduction in their lifespan, which could be detected only after ~50 days of age (post-eclosion), following neuronal (brain)-specific knockdown of either gene (Figures 5C and 6C), whereas their -respective- silencing, specifically in the midgut tissues, resulted in similar to control survival profiles (Figures 5D and 6D).

RNAi-mediated knockdown of *Npc1a* gene in the nervous system (brain) caused an early and significant decline in climbing ability of male flies, which could be readily observed from day 10, post-eclosion (Figure 5E). Intriguingly, neuronal (brain)-specific silencing of *Npc2a* gene in males did not affect their climbing performance, strongly suggesting that *Npc2a* may play a secondary, or redundant, role, compared to *Npc1a* gene, in locomotor function(s) (Figure 6E). Of note, female -transgenic- flies of both genotypes exhibited climbing activities similar to control ones (Figures 5E and 6E). Strikingly, our findings indicate that even moderate reductions of *Npc1a* gene expression are sufficient to impair locomotor performance, in a sex-specific manner, during *Drosophila* aging.

 doi:10.20944/preprints202511.1571.v1

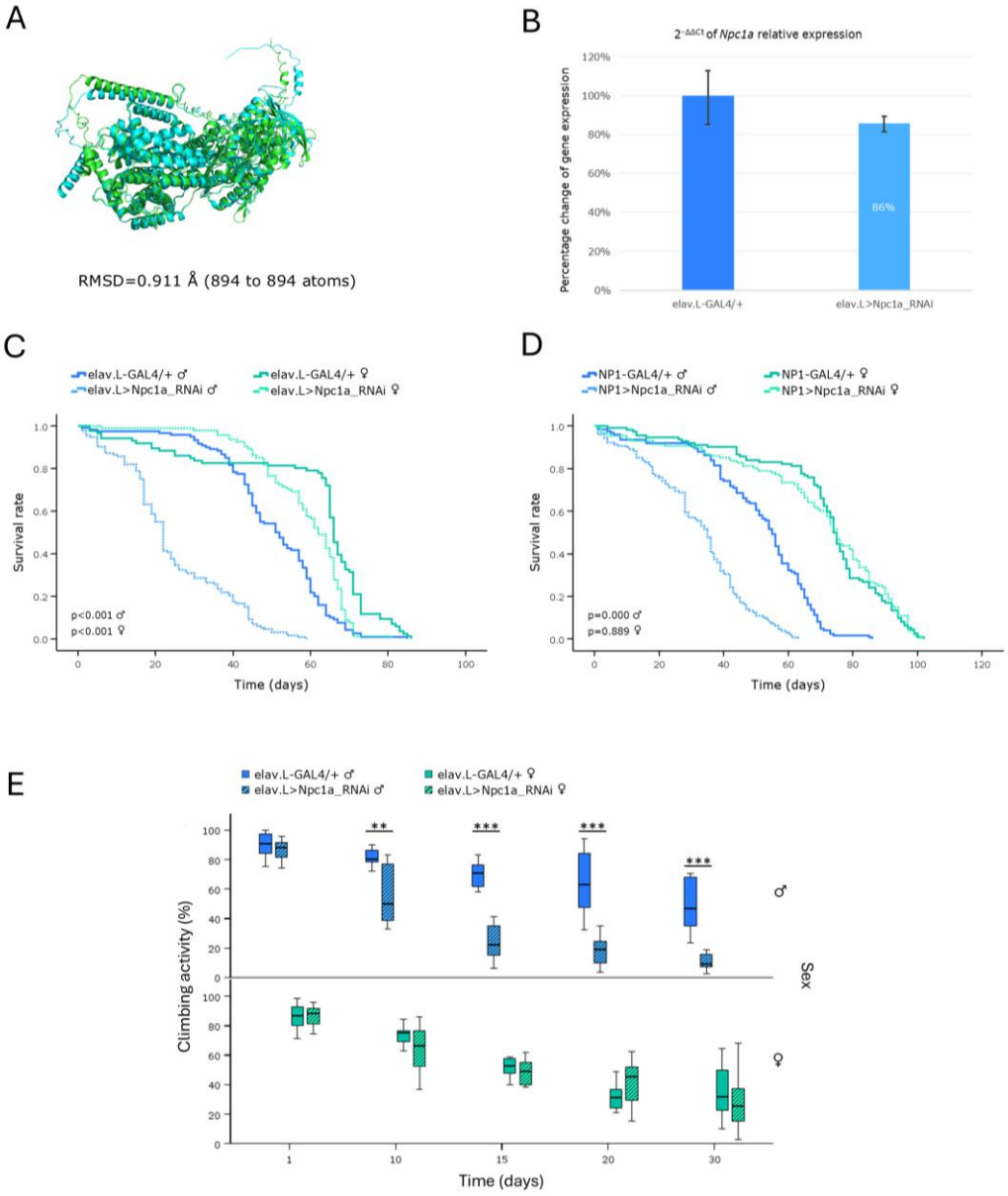

Figure 5. *In vivo* genetic modeling of the Niemann-Pick disease type C1 in *Drosophila*, through targeting of the *Npc1a* ortholog gene, in the brain-midgut axis, during aging. (A) Structural alignment of AlphaFold-derived protein structures of the human *NPC1* (light green) and its *Drosophila* ortholog *Npc1a* (light cyan) genes, being generated and visualized via engagement of the PyMOL molecular graphics system. (B) Relative expression of the *Npc1a* gene in neuronal (brain) tissues of RNAi-targeted flies (elav.L>Npc1a_RNAi), compared to control population (elav.L-GAL4/+), being quantified by real-time qPCR technology. (C) Survival curves of male and female -transgenic- flies, following *Npc1a* gene targeting, specifically in the nervous system (brain). (D) Lifespan profiles of flies that are being typified by midgut-specific *Npc1a* gene silencing (NP1>Npc1a_RNAi). (E) Climbing activity (negative geotaxis) of -transgenic- flies with *Npc1a* gene downregulation, specifically in the nervous system (brain), indicating severe and progressive locomotor decline in *Drosophila* male populations, during aging (0-30 days, post-eclosion). $^{**}p < 0.01$ and $^{***}p < 0.001$.

 doi:10.20944/preprints202511.1571.v1

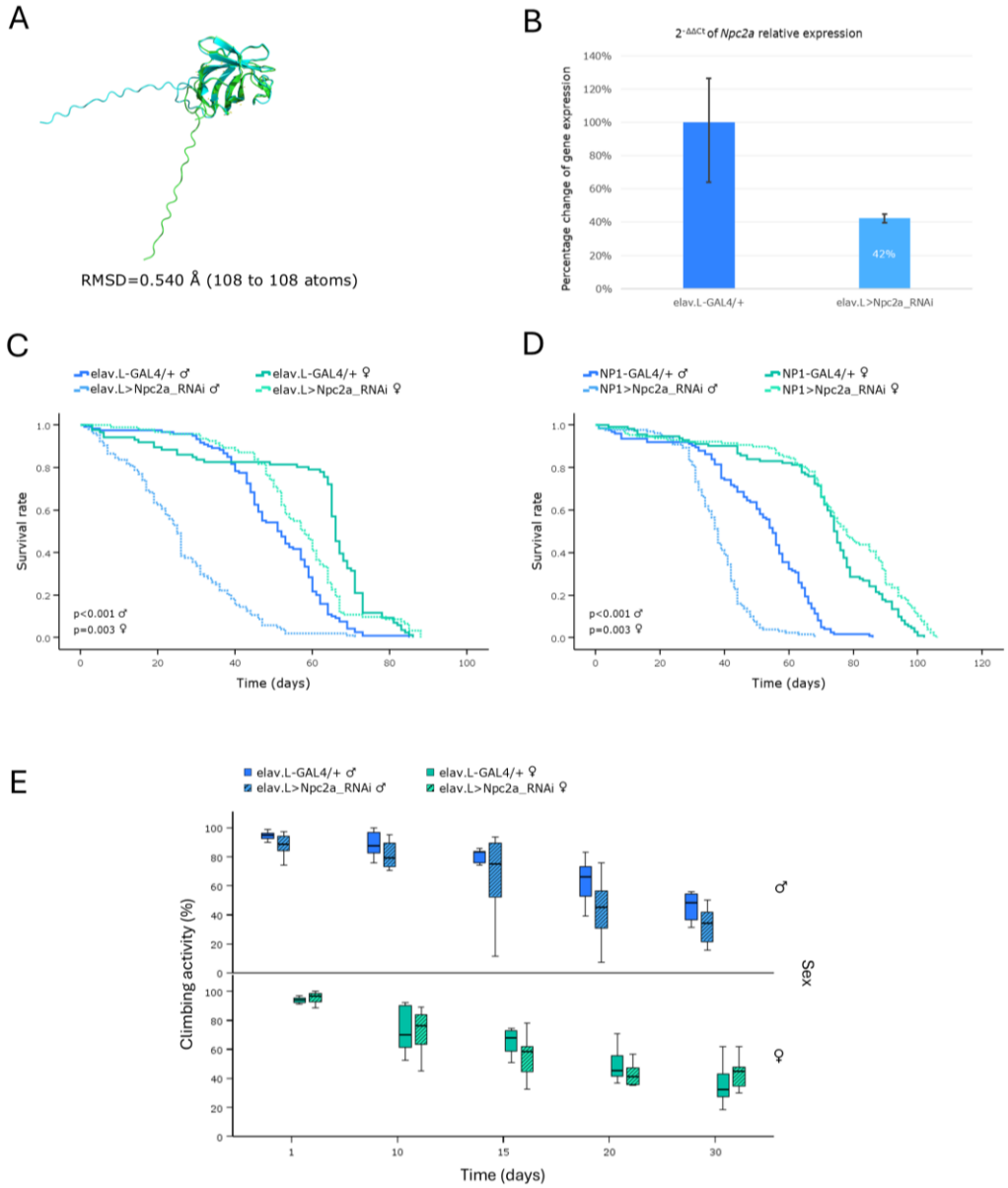

Figure 6. *In vivo* genetic modeling of the Niemann-Pick disease type C2 in *Drosophila*, through targeting of the *Npc2a* ortholog gene, in the brain-midgut axis, during aging. (A) Structural alignment of AlphaFold-derived protein structures of the human *NPC2* (light green) and its *Drosophila* ortholog *Npc2a* (light cyan) genes, with the human reference sequence (NPC2) being aligned to the *Drosophila* protein (Npc2a), using the PyMOL molecular graphics system. (B) Relative expression of the *Npc2a* gene in neuronal (brain) tissues of RNAi-targeted flies (elav.L>Npc2a_RNAi), versus control population (elav.L-GAL4/+), as examined and quantified by real-time qPCR. (C) Lifespan curves of male and female -transgenic- flies being characterized by *Npc2a* gene downregulation, specifically in the nervous system (brain), compared to control population. (D) Survival profiles, after midgut-specific knockdown of the *Npc2a* ortholog gene (NP1>Npc2a_RNAi), compared to control (NP1-GAL4/+). (E) Negative-geotaxis (climbing-activity) assay of flies with neuronal (brain)-specific *Npc2a* gene knockdown, presenting an unimpaired (physiological), age-dependent, decline in motor function(s), compared to controls.

3.3.4. Tay-Sachs/Sandhoff Disease(s)

The GM2 gangliosidoses are caused by defects in the degradation of GM2 ganglioside, leading to its accumulation primarily within neuronal cells. The degradation of GM2 ganglioside requires the lysosomal isoform Hex A, a β-Hexosaminidase enzyme composed of α- and β-subunits being encoded by the *HEXA* and *HEXB* genes, respectively. Mutations in these genes result in the

 doi:10.20944/preprints202511.1571.v1

development of Tay-Sachs (*HEXA*) and Sandhoff (*HEXB*) diseases [10,11]. DIOPT analysis of the *Drosophila* genome identified three putative orthologs encoding β-N-Acetylhexosaminidase-like enzymes; the *Hexo1*, *Hexo2* and *fdl* genes (Table 1). We focused on *Hexo1* and *Hexo2*, as they present the highest sequence homology and significant structural similarity to their human counterparts (Figures 7A and E).

RNAi-mediated knockdown of these genes in the nervous system (brain tissues) caused significant reduction in mRNA expression of ~46% for *Hexo1* (Figure 7B) and ~45% for *Hexo2* (Figure 7F) genes. Neuronal tissue-specific silencing of *Hexo1* ortholog gene led to an age-dependent reduction in the median lifespan of male flies by ~8 days, whereas, in females, it caused a mild increase in early-life survival, followed by a decline in longevity during late(r)-life stages (Figure 7C). In contrast, (pan-)neuronal silencing of *Hexo2* caused a -comparatively- more pronounced decrease in median lifespan by ~26 days, for male flies, and by ~11 days, for female populations (Figure 7G). Notably, RNAi-mediated downregulation of each gene in the midgut tissues proved to induce no significant impact on the lifespan profile of either gender (Figures 7D and H), thereby suggesting a limited, or redundant, functional role for *Hexo1* and *Hexo2* genes in *Drosophila* midgut environment, during aging.

Taken together, the RNAi transgenic lines used in this study proved capable to recapitulate key pathological features of sphingolipidoses, thus reinforcing the exploitation of *Drosophila* as a reliable and powerful model organism, for unmasking the molecular underpinnings of sphingolipidoses and related LSD pathologies, during aging.

 doi:10.20944/preprints202511.1571.v1

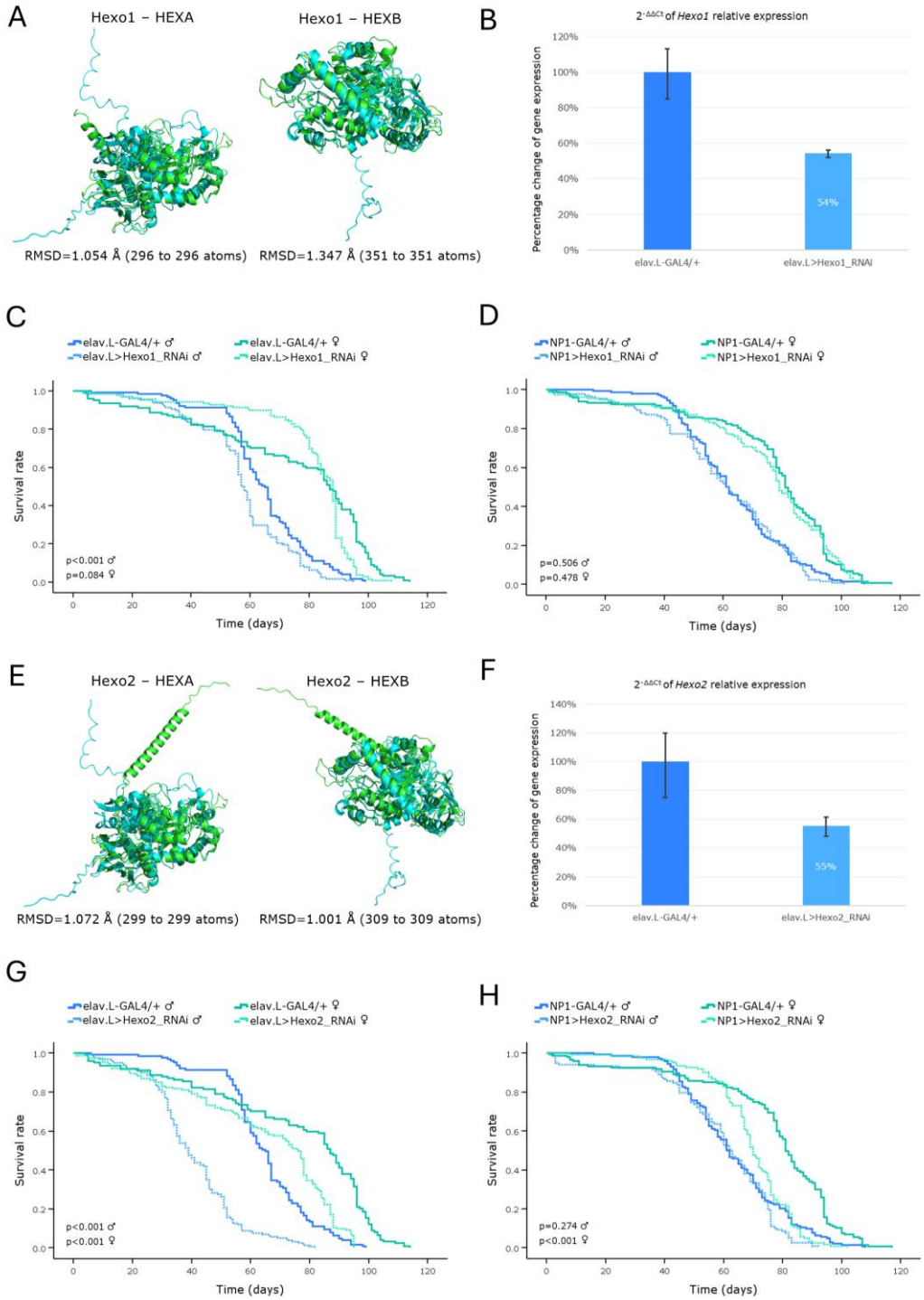

Figure 7. Genetic modeling of Tay-Sachs and Sandhoff diseases, via targeting their *Drosophila* ortholog genes, in the brain-midgut axis, during aging, *in vivo*. (A-D) Functional analysis of *Hexo1* gene: (A) Alignment of AlphaFold-derived molecular structures of the proteins produced by human *HEXA* and *HEXB* genes (light green) with their *Drosophila* ortholog protein being encoded by the *Hexo1* gene (light cyan), using the PyMOL molecular graphics system. (B) Relative expression levels of the *Hexo1* gene in neuronal (brain) tissues of RNAi-targeted flies (elav.L>Hexo1_RNAi), compared to controls (elav.L-GAL4/+), as measured and quantified by real-time qPCR technology. (C) Survival curves of -transgenic- male and female flies, following nervous system (brain)-specific knockdown of *Hexo1* gene, compared to controls. (D) Lifespan profiles, after *Hexo1*-gene knockdown, specifically in midgut tissues (NP1>Hexo1_RNAi), compared to control (NP1-GAL4/+). (E-H) Functional analysis of *Hexo2* gene: (E) Structural alignment of AlphaFold-predicted protein structures being derived from human *HEXA* and *HEXB* genes (light green), and the *Drosophila* ortholog protein synthesized by

 doi:10.20944/preprints202511.1571.v1

the *Hexo2* gene (light cyan). (F) Relative expression levels of *Hexo2* gene in transgenic flies over-expressing the *Hexo2*^{RNAi} species, specifically in the nervous system (brain) (elav.L>Hexo2_RNAi), versus control populations (elav.L-GAL4/+), via real-time qPCR technology employment. (G) Survival curves of male and female flies being characterized by (pan-)neuronal *Hexo2* knockdown, compared to control conditions. (H) Lifespan profiles, after *Hexo2*-gene silencing, specifically in the midgut tissues (NP1>Hexo2_RNAi), compared to control (NP1-GAL4/+).

3.4. Modeling of Pompe Disease in Drosophila

3.4.1. Pompe Disease

Pompe disease is a glycogen storage disorder caused by a deficiency in Lysosomal acid-a-Glucosidase, which is encoded by the *GAA* gene, and leads to intra-lysosomal glycogen accumulation [6]. In *Drosophila*, there is no single direct ortholog of the human *GAA* gene, hitherto, pinpointed. However, three homolog genes can be, *in silico*, identified; *GCS2alpha*, which has a moderate DIOPT score, and *tobi* and *CG33080*, which show low homology values (Table 1). For our study, we selected *GCS2alpha* gene, as its cognate protein is being presented with the -comparatively- highest (predicted) homology and structural similarity to its human counterpart (Figure 8A). Furthermore, we also included *tobi* gene (Figure 8E), due to its relatively higher DIOPT score, compared to the *CG33080* respective one. The gene-silencing efficiency of our RNAi-based strategy, using a neuronal-specific driver, proved significantly strong for both ortholog genes, as the reduction in mRNA expression level was measured at ~63% for *GCS2alpha* (Figure 8B) and at ~64% for *tobi* (Figure 8F) gene, versus control conditions. Neuronal (brain)-specific knockdown of *GCS2alpha* caused a significant decrease of lifespan in male flies, a major pathology that was clearly detected from early adulthood (Figure 8C). Regarding *tobi*, its downregulation in males was linked to an age-dependent phenotype typified by reduced viability being observed after ~40 days from hatching (Figure 8G). Intriguingly, female flies did not present any negative effect on lifespan, after silencing of either gene in the nervous system (Figures 8C and G). In fact, *tobi* knockdown was shown to rather improve than deteriorate female viability (Figure 8G). Our data strongly suggest for the sexually dimorphic contribution of *GCS2alpha* and *tobi* genes to tightly controlling lifespan in *Drosophila*. Nevertheless, midgut-specific silencing of *GCS2alpha* or *tobi* gene did not seem to cause any significant effect on life expectancy in either gender, strongly supporting their (*GCS2alpha* and *tobi*) predominant functional involvement in the nervous (brain), but not midgut, system, during *Drosophila* aging (Figures 8D and H).

 doi:10.20944/preprints202511.1571.v1

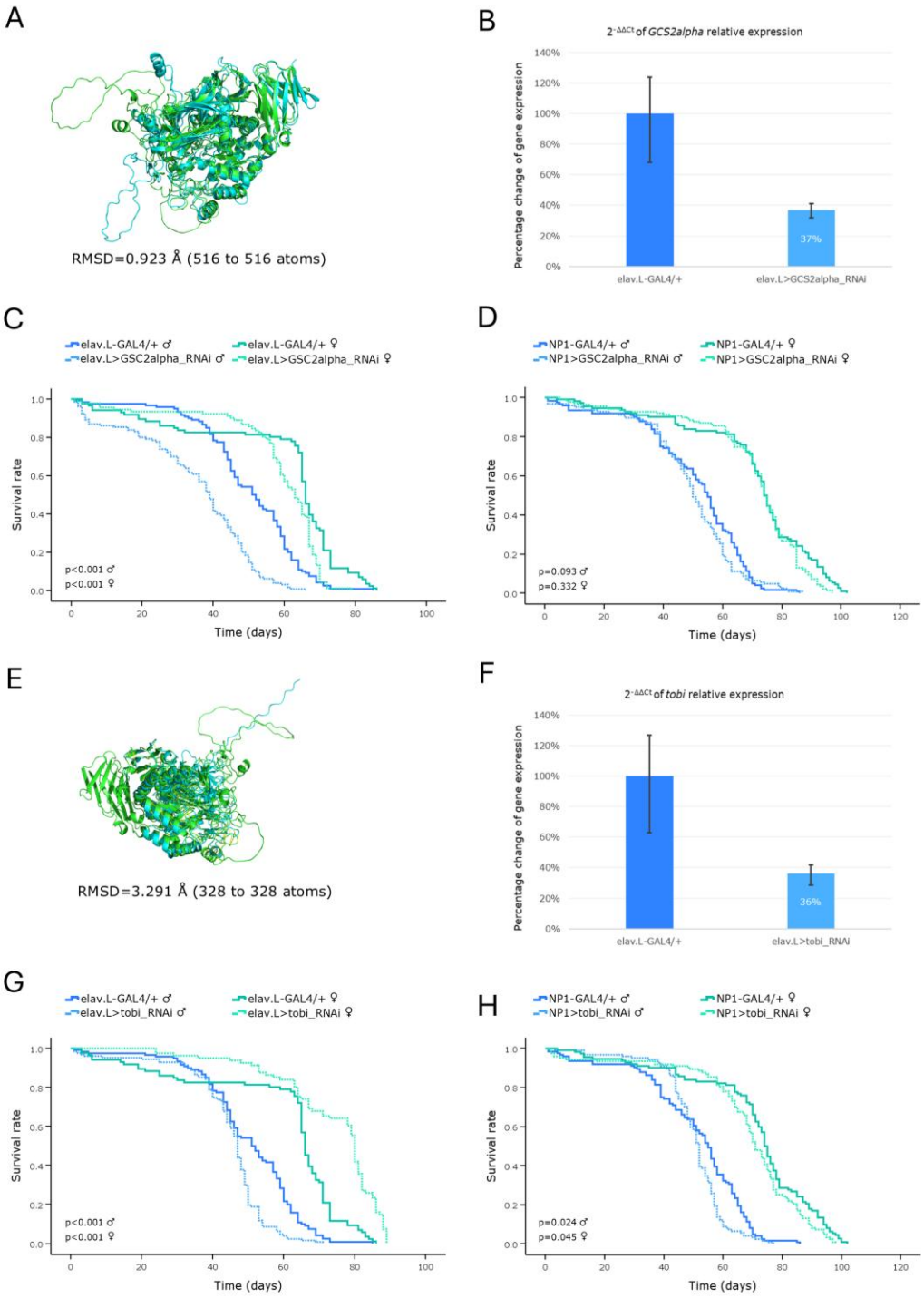

Figure 8. Modeling of Pompe disease-related orthologs in *Drosophila* brain-midgut axis, during aging. (A-D) Functional analysis of the *GCS2alpha* gene: (A) Structural alignment of AlphaFold-derived, superimposed, protein products of the human *GAA* (light green) and the *Drosophila* ortholog *GCS2alpha* (light cyan) genes, being generated and visualized using the PyMOL molecular graphics system. (B) Relative (endogenous) *GCS2alpha* mRNA expression levels in neuronal (brain) tissues of RNAi-targeted flies (elav.L>GCS2alpha_RNAi), compared to controls (elav.L-GAL4/+), measured and quantified by real-time qPCR. (C) Survival curves of male and female flies, following (pan-)neuronal *GCS2alpha*-gene knockdown, versus control conditions. (D) Lifespan profiling, after *GCS2alpha*-targeted downregulation, specifically in *Drosophila* midgut tissues (NP1>GCS2alpha_RNAi), compared to control (NP1-GAL4/+). (E-H) Functional analysis of the *tobi* gene: (E) Structural alignment of AlphaFold-derived, superimposed, protein products of the human *GAA* (light green) and the *Drosophila* ortholog *tobi* (light cyan) genes, via PyMOL engagement. (F) Relative (endogenous) *tobi*

 doi:10.20944/preprints202511.1571.v1

mRNA expression levels in neuronal (brain) tissues, after specific downregulation of *tobi* gene in the nervous system (brain) (elav.L>tobi_RNAi), versus control fly population (elav.L-GAL4/+), via real-time qPCR platform engagement. (G) Survival curves of male and female flies, being characterized by nervous system (brain)-specific *tobi*-gene knockdown, compared to control conditions. (H) Viability profiles of, male and female, transgenic flies, after *tobi*-gene silencing, specifically in *Drosophila* midgut tissues (NP1>tobi_RNAi), versus control, respective, genetic crosses (NP1-GAL4/+).

3.5. Modeling of Mucopolysaccharidoses in Drosophila

Mucopolysaccharidoses (MPSs) are caused by deficiencies in specific lysosomal hydrolases responsible for the sequential degradation of one or more glycosaminoglycans (GAGs), thus resulting in their lysosomal accumulation and ultimately cellular dysfunction [8].

3.5.1. Hurler Syndrome

Hurler syndrome, or MPS type I, is caused by a deficiency in α-L-Iduronidase (encoded by the *IDUA* gene), leading to the pathological storage of dermatan and heparan sulfate inside the lysosomes of a wide range of tissues [13]. In *Drosophila*, DIOPT analysis identified *Idua* as the single ortholog of human *IDUA* gene, with a high-confidence homology score (Table 1) and an RMSD value of 1.123 Å (Figure 9A). Neuronal-specific RNAi-mediated knockdown of *Idua* gene caused a ~30% reduction in gene expression (Figure 9B), which proved sufficient to induce a pathological phenotype in male flies. These transgenic males exhibited a severely shortened lifespan (Figure 9C), with their median survival being reduced by ~24 days, and impaired climbing ability commencing as early as day one of their adult life (Figure 9E). Strikingly, high mortality rates prevented the inclusion of 30-day-old male flies in the climbing assay, due to insufficient sample size. In contrast, female transgenic flies were characterized by absence of statistically significant changes in either life expectancy (Figure 9C) or climbing activity, apart from a slight improvement in locomotor performance observed at -approximately- day 30 (post-eclosion) (Figure 9E). Of note, midgut-specific knockdown of the *Idua* gene resulted in mildly reduced survival, for both transgenic fly sexes, compared to controls (Figure 9D).

Altogether, the, herein, obtained results demonstrate that, following *Idua* suppression, *Drosophila* manifests key neurological and viability-related pathologies, which represent phenotypes indicative of human Hurler syndrome, thereby highlighting the strong potential of "fly-*Idua*^{RNAi}" genetic platform to serve as a reliable and effective *in vivo* -animal- disease model, for mechanistically investigating Hurler syndrome pathogenesis, and pre-clinically supporting high-throughput drug-screening systems, towards the discovery of novel therapeutic schemes and regimens.

 doi:10.20944/preprints202511.1571.v1

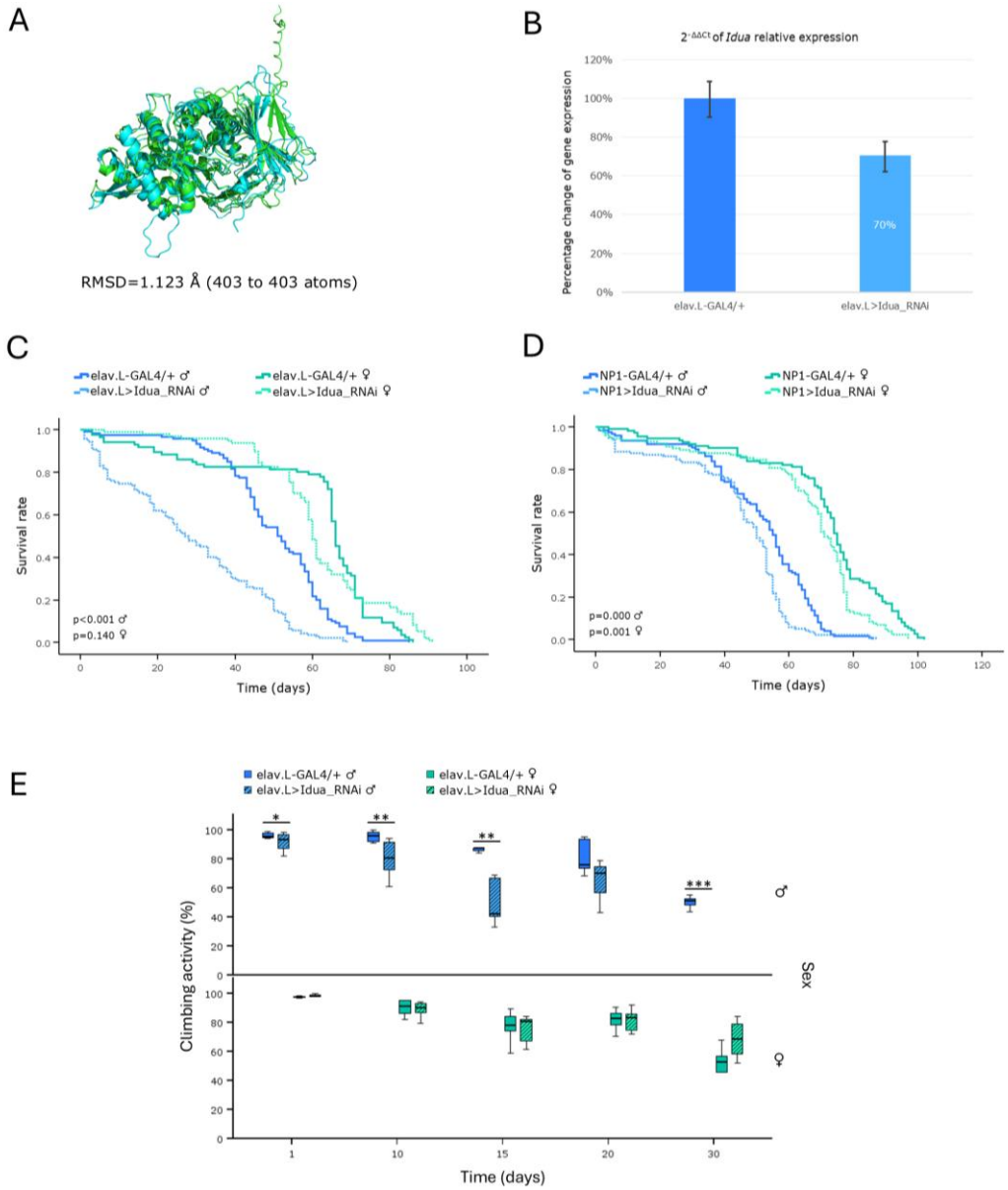

Figure 9. *In vivo* genetic modeling of Hurler syndrome in *Drosophila*, via the *Idua* ortholog gene targeting, in the brain-midgut axis, during aging. (A) Structural alignment of AlphaFold-derived protein, superimposed, structures being encoded by the human *IDUA* (light green) and its *Drosophila* ortholog *Idua* (light cyan) -respective- genes, generated and visualized via the PyMOL molecular graphics system. (B) Relative expression levels of the *Idua* gene in neuronal (brain) tissues of RNAi-targeted flies (elav.L>Idua_RNAi), versus control ones (elav.L-GAL4/+), suitably quantified via the real-time qPCR technology engagement. (C) Survival curves of male and female, transgenic, flies, following *Idua* gene downregulation, specifically, in the nervous system (brain), compared to controls. (D) Viability profiles, after midgut-specific silencing of the *Idua* gene (NP1>Idua_RNAi), versus control conditions (NP1-GAL4/+). (E) Climbing performance of flies with neuronal (brain)-specific knockdown of the *Idua* gene (elav.L>Idua_RNAi), compared to control genetic crosses (elav.L-GAL4/+). *$p < 0.05$, **$p < 0.01$ and ***$p < 0.001$.

3.5.2. Hunter Syndrome

Hunter syndrome, or MPS type II, is a rare X-linked recessive disorder caused by functional deficiency of the lysosomal enzyme Iduronate-2-sulfatase (encoded by the *IDS* gene, in humans), which is critical for the catabolism of certain glycosaminoglycans (GAGs); the dermatan- and heparan-sulfate -GAG- species [14]. In *Drosophila*, a single ortholog gene, the *Ids*, can be identified in the 3rd chromosome, with a high DIOPT score (Table 1) and a strong structural similarity of its protein

 doi:10.20944/preprints202511.1571.v1

product to the human protein counterpart (RMSD value as low as 0.473 Å; Figure 10A). Targeted, RNAi-mediated, knockdown of the *Ids* gene, specifically, in neuronal (brain) cells led to ~26% reduction in mRNA expression levels (Figure 10B). Despite this modest downregulation, male flies were presented with an age-dependent decrease in life expectancy, with their median survival being reduced by ~18 days, compared to control males (Figure 10C). In contrast, female flies were largely unaffected, producing survival curves comparable to those of the control populations (Figure 10C).

Similarly, tissue-specific knockdown of the *Ids* gene in *Drosophila* midgut tissues did not seem to significantly affect the lifespan profile of either fly-sex setting (Figure 10D), further emphasizing the functional importance of *Ids* gene product, specifically, in the central nervous system (CNS). It may be the remaining *Ids* activity, of ~74%, that lies near a functional threshold being capable to sufficiently maintaining viability in female, but not male, fly populations, during aging.

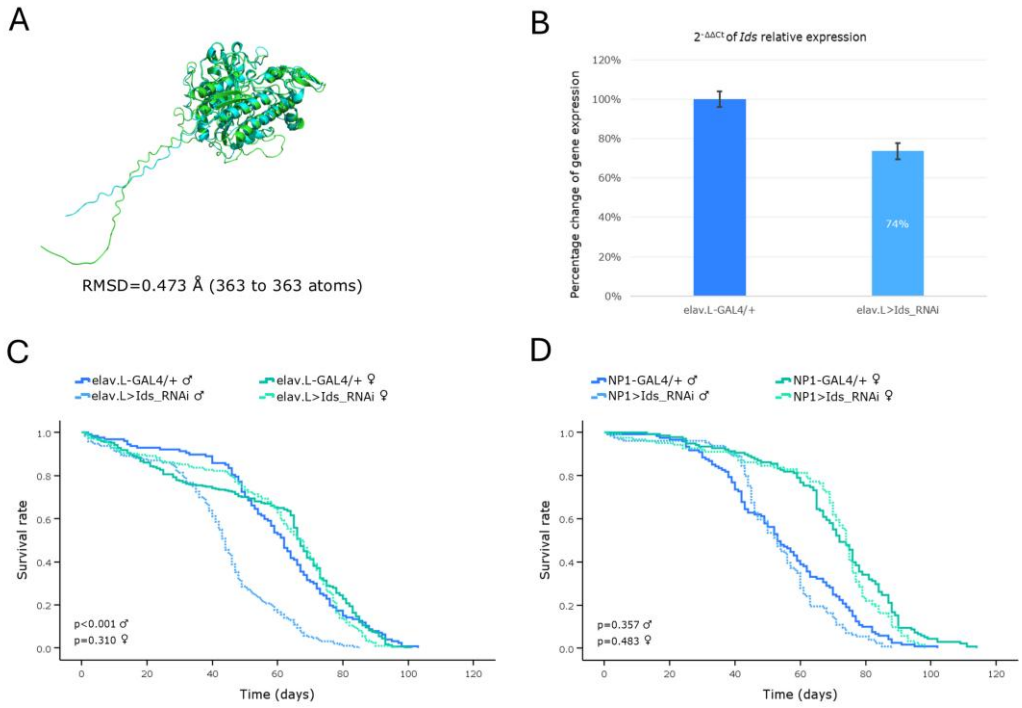

Figure 10. *In vivo* genetic modeling of Hunter syndrome in *Drosophila*: RNAi-mediated targeting of the *Ids* ortholog gene, in the brain-midgut axis, during aging. (A) Structural alignment of the AlphaFold-predicted, superimposed, protein structures being derived from the human *IDS* (light green) and its *Drosophila* ortholog *Ids* (light cyan) genes. Human protein was aligned to the *Drosophila* structure, using the PyMOL molecular graphics system. (B) Relative expression levels of the (endogenous) *Ids* gene, specifically, in neuronal (brain) tissues of RNAi-targeted flies (elav.L>Ids_RNAi), compared to controls (elav.L-GAL4/+), suitably quantified by real-time qPCR technology. (C) Survival curves of transgenic flies from both sexes, following *Ids* gene knockdown, specifically, in the nervous system (brain) (elav.L>Ids_RNAi), versus control conditions (elav.L-GAL4/+). (D) Lifespan profiles of male and female -transgenic- flies, after *Ids* gene silencing, specifically, in midgut tissues (NP1>Ids_RNAi), compared to control genetic crosses (NP1-GAL4/+).

3.5.3. Sly Disease

Sly disease, or MPS type VII, is an autosomal recessive LSD caused by mutations in the human *GUSB* gene, which encodes the β-Glucuronidase enzyme. Loss of this enzyme leads to the accumulation of undegraded, or partially degraded, glycosaminoglycans (GAGs), ultimately resulting in widespread cellular dysfunction [14]. In *Drosophila*, three orthologs of the human *GUSB* gene have been identified. Among them, *CG15117* exhibits the highest DIOPT score (Table 1) and a notably low RMSD value of 0.598 Å (Figure 11A), indicative of their strong structural similarity. In the, herein, developed *Drosophila* model of Sly disease, RNAi-mediated knockdown of the *CG15117*

 doi:10.20944/preprints202511.1571.v1

gene, specifically, in the nervous system (brain) revealed a modest reduction, of ~39%, in mRNA expression levels (Figure 11B). Male transgenic flies with neuronal (brain)-specific downregulation of *CG15117* gene were characterized by an age-dependent decline in lifespan, with a median reduction of ~16 days, compared to control males (Figure 11C). In contrast, female transgenic flies were presented with similar-to-control survival curves, under the same growth conditions (Figure 11C).

Interestingly, midgut-specific knockdown of the *CG15117* gene, also, caused a pronounced, sex-dependent, lifespan impairment pattern. Male transgenic flies presented a significantly shortened lifespan, as clearly indicated by their reduced median and maximum lifespan of ~25 and ~40 days, respectively (Figure 11D). Female transgenic flies were (comparatively) less affected, with only a slight decrease in maximum lifespan being observed, thereby suggesting a male-specific vulnerability to *CG15117* loss in both neuronal (brain) and midgut tissues. Negative-geotaxis (climbing-activity) assay of RNAi-mediated, *CG15117*-targeted, flies, specifically in the nervous system (brain), unveiled a progressive, age-dependent, decline in locomotor activity, for both sexes (Figure 11E). Although *CG15117*-downregulated flies presented near to normal climbing activity during the initial days of adult life, with only a mild early decline being observed in females, their motor performance deteriorated significantly from day 10 onward. By this stage, their climbing efficiency closely resembled that of 20-day-old control flies, thereby indicating an accelerated onset of age-dependent locomotor impairment (Figure 11E).

 doi:10.20944/preprints202511.1571.v1

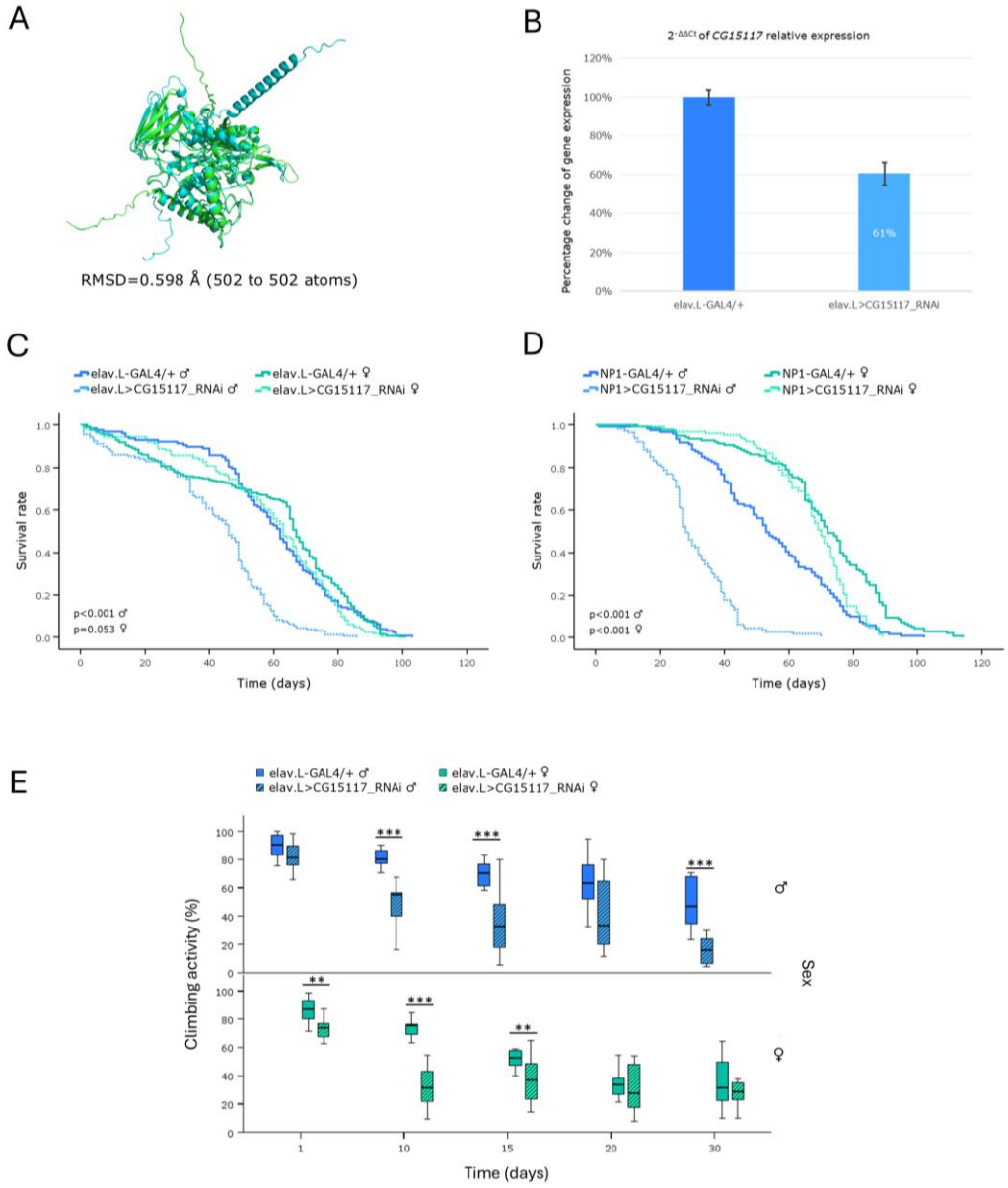

Figure 11. *In vivo* genetic modeling of Sly disease in *Drosophila*, via the *CG15117* ortholog gene targeting, in the brain-gut axis, during aging. (A) Structural alignment of AlphaFold-derived, superimposed, protein structures being encoded by the human *GUSB* (light green) and its *Drosophila* ortholog *CG15117* (light cyan) genes, generated and visualized using the PyMOL molecular graphics system. (B) Quantitative analysis of the *CG15117* mRNA levels, specifically, in neuronal (brain) tissues of $CG15117^{RNAi}$-(over-)expressing flies (elav.L>CG15117_RNAi), compared to controls (elav.L-GAL4/+), via the real-time qPCR technology engagement. (C) Lifespan curves of male and female -transgenic- flies, following nervous system (brain)-specific targeting of the *CG15117* gene (elav.L>CG15117_RNAi), compared to control conditions (elav.L-GAL4/+). (D) Survival profiles of transgenic flies (both sexes) with targeted *CG15117*-gene knockdown, specifically, in midgut tissues (NP1> CG15117_RNAi), compared to control genetic crosses (NP1-GAL4/+). (E) Climbing performance of transgenic flies with neuronal (brain)-specific *CG15117*-gene downregulation (elav.L>CG15117_RNAi), versus control genetic settings (elav.L-GAL4/+), measured and quantified over time (0-30 days, post-eclosion) (using the negative-geotaxis assay), demonstrating the progressive, age- and sex-dependent, impairment in motor function(s). $^{**}p < 0.01$ and $^{***}p < 0.001$.

Taken together, the majority of the, herein, developed *Drosophila* models of Mucopolysaccharidoses (MPSs) successfully recapitulate key pathological features of MPS disorders, such as shortened lifespan and progressive motor decline. These invertebrate models provide a

 doi:10.20944/preprints202511.1571.v1

powerful platform for conducting genetic screens, *in vivo*, to: (a) mechanistically illuminating MPSs, (b) identifying genetic modifiers, and (c) conducting rapid, reliable, comprehensive and cost-effective drug-screening trials that are unfeasible to be implemented in -typical- vertebrate (e.g., zebrafish and mouse) model organisms.

4. Discussion

Most Lysosomal Storage Disorders (LSDs) lack effective treatments, rendering genome editing one of the most promising therapeutic strategies. However, before these genome editing tools can be applied in humans, several critical steps must precede, ranging from *in vitro* testing to clinical trials. To maximize safety and gather extensive preliminary data, *in vivo* modeling, using invertebrates, has gained major attention in the recent years [15,17]. These organisms offer a wide array of genetic tools and allow the *in vivo* study of various biological pathways and therapeutic approaches, in shorter times and with fewer ethical concerns than those in mammals. *Drosophila melanogaster* is a well-established invertebrate model system that offers an ideal background for genetic and biological studies of different human pathologies, as it contains functional orthologs for ~75% of the human disease-related genes [31]. *Drosophila* also features a plethora of genetic tools, including the GAL4/UAS, CRISPR/Cas9 and RNAi molecular platforms, which allow cell/tissue-specific gene targeting/downregulation [32,33].

In the present study, we suitably employed the -binary- GAL4/UAS and RNAi genetic systems, to selectively knockdown fly orthologs of human LSD-related genes, along the brain-midgut axis, during aging. Employment of commercially available transgenic strains, directly obtained from Bloomington *Drosophila* Stock Center (BDSC; Indiana, USA), enabled us to systemically investigate their morbid effects, *in vivo*. These findings provide a powerful invertebrate model for future studies, to broadly explore and deeply comprehend the molecular mechanisms that control LSD-pathology (initiation and progression), and to successfully develop novel genetic- and drug-based strategies for LSD-targeting therapies.

Sphingolipidoses represent a sub-category of LSDs being developed by deficiencies in enzymes responsible for the catabolism of sphingolipids, and they mainly affect nervous-system and peripheral-organ tissues. Gaucher disease (GD) is the most prevalent form and derives from deficiencies in the β-Glucocerebrosidase (GBA1) enzyme, leading to toxic accumulation of glucosylceramide [10]. Utilization of mouse models for Gaucher disease (GD) has proven challenging and limited, due to the elevated perinatal lethality associated with *GBA1* gene mutations [10,34].

Hence, towards the establishment of a new *in vivo* model for the disease (GD), we, herein, investigated the impact of downregulating the *Drosophila Gba1a* and *Gba1b* orthologs of human *GBA1* gene, along the brain-midgut axis, during aging. Our results revealed a marked reduction in lifespan and climbing ability, with females being more severely affected, compared to male populations. A previous study of *Drosophila* Minos-insertion mutants of the *GBA1* orthologs reported that *Gba1b* mutants exhibited shortened lifespan and impaired climbing ability, whereas *Gba1a* mutants did not present significant pathologies [35]. Although *Drosophila Gba1a* and *Gba1b* fly orthologs show differential tissue-expression patterns, with *Gba1a* being primarily expressed in the midgut, and *Gba1b* being detected in the adult head and fat body [36], both genes seem to affect fly longevity and kinetic ability in a similar pattern, when downregulated in brain and midgut tissues.

Therefore, our approach indicates that both genes are essential for motor performance and survival in *Drosophila*. The progressive loss of neuronal cells and the resulting neurotoxicity in Gaucher disease (GD) [10] likely underlie the observed pathologies in locomotor activity and lifespan. The, herein, identified sex-specific differences in our *Drosophila* Gaucher disease (GD) model system may arise from multiple factors, including hormonal regulation, metabolic programs, immune responses and reproductive properties [37–39]. Taken together, our findings strongly support *Drosophila* as a powerful and versatile *in vivo* model for Gaucher disease (GD), providing insights into its genetic and pathophysiological mechanisms, including sex-specific disease manifestations.

 doi:10.20944/preprints202511.1571.v1

Fabry is an X-linked recessive sphingolipidosis caused by a deficiency in the lysosomal enzyme α-Galactosidase A, due to mutations in the human *GLA* gene [7]. Interestingly, in our model system, herein being investigated, genetic downregulation of the fly *GLA* ortholog, *CG5731*, proved capable to more severely affect female flies, in both life expectancy and climbing capacity, compared to male populations. Of note, the sex-linked inheritance pattern having been observed in humans cannot be directly applied in *Drosophila*, since male flies upregulate their single X chromosome via dosage compensation [40] and, additionally, *CG5731* is not an X-linked gene. A mechanistic explanation for the -comparatively- increased sensitivity detected in female flies may be associated with gender- and/or tissue-specific gene-expression programs, and differences in metabolic/nutritional demands and/or hormonal pathway/network activities. Moderate homologies might also reflect redundant or compensatory functions by other enzymes, or alternative mechanisms, in *Drosophila* that are absent or less efficient in humans. In a mouse model of the disease (FD), both male and female mice, deficient in α-Gal A (α-Galactosidase A), manifested a clinically normal phenotype at the 10^{th}-14^{th} weeks of age, thus rendering Fabry-disease (FD) modeling, in this vertebrate/mammalian system, challenging and limited [41]. However, in a study of *Drosophila* transgenic populations, expressing the human mutant *GLA* (variant) forms A156V and A285D, significant locomotor dysfunction and reduced lifespan were observed, compared to control flies (expressing the human wild-type enzyme). Strikingly, these phenotypes could be ameliorated with Migalastat (Fabry disease -FD- medication) treatment [42].

Altogether, our RNAi-based genetic platform, which targets the endogenous expression of *CG5731* fly gene (human *GLA* homolog), specifically in the brain-midgut axis, during aging, may offer a powerful, reliable, multifaceted, dynamic and sensitive *in vivo* model system, for comprehensively studying Fabry disease (FD), to enabling efficient drug screening and to illuminating underlying disease mechanisms.

Niemann-Pick type C disease (NPC) is a neurodegenerative disorder that is sub-divided into types C1 and C2, depending on the respective -human- gene (*NPC1* or *NPC2*) that is mutated. It is characterized by abnormalities in the intracellular transport of endocytosed cholesterol, which leads to the accumulation of cholesterol and sphingolipids within endo-lysosomes [6,12]. In the present study, we investigated the consequences of RNAi-mediated knockdown of *Drosophila Npc1a* and *Npc2a* gene orthologs, suitably engaging the GAL4/UAS genetic system, along the brain-midgut axis, during aging. The obtained male -transgenic- flies were characterized by reduced lifespan and locomotor dysfunction, for either organ-specific (brain, or midgut) targeting, in contrast to the female flies, which exhibited near-to-normal phenotypes.

A previous study in *Drosophila*, using loss-of-function mutants of the *Npc1a* gene, revealed developmental arrest at the first larval stage [43], thus rendering age-dependent pathologies during adulthood impossible to be profiled. Strikingly, in our model, although the viability patterns for the two genes are largely similar, the relative expression of *Npc1a* gene was detected less markedly reduced, compared to the *Npc2a* respective one (Figures 5B and 6B). This indicates that even a modest decrease in the *Npc1a* gene-expression levels, within the nervous system (brain) setting, is sufficient to trigger a pathological phenotype, thereby highlighting the *Npc1a* essential role(s) in *Drosophila* well-being, during aging.

In toto, our genetic approach provides a powerful, trustworthy and manageable model system, for mechanistically illuminating and therapeutically advancing Niemann-Pick type C disease (NPC), *in vivo*.

GM2 gangliosidoses are characterized by excessive accumulation of ganglioside -GM2- species and related glycolipids in the lysosomes. The main forms include Tay-Sachs disease (TSD), caused by mutations in the *HEXA* gene, and Sandhoff disease (SD), caused by mutations in the *HEXB* gene [9–11]. In *Drosophila*, three genes (*Hexo1*, *Hexo2* and *fdl*) have been identified, as encoding β-Hexosaminidase-like enzymes, based on sequence homologies to human Hexosaminidases [44,45]. Strikingly, RNAi-mediated downregulation of the *Hexo2* (but not *Hexo1*) gene, specifically in the brain, revealed a remarkable reduction in life expectancy of *Drosophila* -transgenic- male flies (Figure

 doi:10.20944/preprints202511.1571.v1

7G). Given that GM2 gangliosidoses are known to predominantly affect the central nervous system (CNS) [10,11], our results point to the essential contribution of -certain- β-Hexosaminidases to neuronal development and CNS/brain functionality in *Drosophila*, during aging, thereby validating model's relevance to molecularly investigating GM2 gangliosidoses-induced neuro-pathologies, *in vivo*.

Mucopolysaccharidoses (MPSs) comprise a class of 11 lysosomal storage disorders, with each one being derived from -driver- deficiency in the activity of a distinct lysosomal hydrolase; they all belong to a family of enzymes that are critically involved in the sequential degradation of glycosaminoglycans (GAGs). MPS I and MPS II sub-types were typically classified among the first syndromes identified within this group [8]. In our Hurler syndrome (HLS) (MPS I; α-L-Iduronidase deficiency) *in vivo* model, although the expression of *IDUA* gene is not severely downregulated, reduced lifespan and locomotor deficiency, along the brain-midgut axis, were observed. Of note, a distinct study, regarding Hurler-syndrome (HLS) modeling, using a similar strategy, but different RNAi strains, which can still target the same *Drosophila IDUA* ortholog (*CG6201*) gene, has been previously reported by Filippis *et al*. [46]. However, in their set of experiments, although flies with reduced expression of the *IDUA* gene, in neuronal and glial cells, were presented with locomotion deficiencies, they, unexpectedly, manifested a longer lifespan, compared to controls [46].

Hence, our *Drosophila* Hurler-syndrome (HLS) model represents an invaluable, powerful, informative, constructive, manageable, novel, and, also, complementary (to the existing) -biological-tool, for genetically dissecting disease mechanisms and systemically expanding the repertoire of -experimental- *in vivo* models, hitherto available, to deeper investigating Hurler-syndrome (HLS) pathology, both mechanistically and therapeutically, for human's maximum benefit.

Hunter syndrome (HNS) (MPS II; Iduronate-2-sulphatase deficiency) is an X-linked recessive LSD. Remarkably, in our -invertebrate- model system, only males exhibited a notable reduction in life expectancy, a pathological phenotype that is genetically associated with the sex-dependent nature of the (HNS) disease, in humans. The genetic modeling of Hunter syndrome (HNS) in *Drosophila* has been previously described, using the same ("RNAi") strains, with the authors concluding that residual *Ids*/Ids activity(ties) may be sufficient to rescue MPS II-related pathologies, since, in their lethality assays, the survival from larva to pupa and the metamorphosis to the adult phase were not affected [47]. In contrast to their argument that engagement of RNAi-dependent -transgenic-technology for MPS II knockdown is not an effective strategy, our data strongly suggest that, under certain circumstances and specific settings, the exploitation of male flies, as a novel and reliable model system, for Hunter syndrome (HNS)-pathology research, *in vivo*, should not be ignored, or disregarded.

Employment of our Sly-disease (SLD) (MPS VII; β-Glucuronidase deficiency) -LSD- model demonstrated a remarkable reduction in the viability of male flies, along the brain-midgut axis, together with a progressive decline in locomotor activity for both sexes, during aging. A *Drosophila* model of MPS VII, developed by knocking-out the *CG2135* gene, the fly ortholog of human *GUSB*, has been previously established, by Bar *et al*., successfully recapitulating key features of the Sly disease (SLD), such as shortened lifespan, motor deficiencies and neurological abnormalities [48]. Notably, *Drosophila* possesses two orthologs of the human *GUSB* gene; the *CG2135* (*βGlu*) and the *CG15117*, with the latter exhibiting a slightly higher similarity score in DIOPT [25]. Although Bar *et al*. found that CG15117 was 6-fold less active than CG2135, our results clearly demonstrate that targeted downregulation of *CG15117*, in either brain or midgut tissues, during aging, critically compromises male fly viability, thereby strongly suggesting its (*CG15117*) beneficial utilization as an additional, but important and powerful, screening tool, for Sly disease (SLD) research, *in vivo*.

Altogether, we have, herein, identified the *Drosophila* orthologs of genes that are responsible for the most common Lysosomal Storage Disorders (LSDs), in humans, and systematically screened them for "patho-phenotypic" effects on life expectancy and climbing proficiency, specifically within the brain-midgut axis, during aging, suitably engaging the GAL4/UAS -binary- transgenic system, in combination with the RNAi-mediated gene-silencing platform. Most of these, *in vivo*, LSD models in

 doi:10.20944/preprints202511.1571.v1

Drosophila, herein, proved capable to successfully recapitulate key-disease phenotypes being identified in humans, including significantly reduced lifespan and progressive climbing deficiency, which serve as proxy for neuro-muscular disintegration, in age- and sex-dependent manners.

These -consistent- phenotypic parallels undoubtedly underline the value and importance of *Drosophila* as a robust, reliable, powerful, rapid, multifaceted, versatile and manageable, invertebrate, model system, ideally suitable and exploitable, for high-throughput genetic and pharmacological, *in vivo*, screenings, aiming at pathological-phenotype(s) rescue(s), while, also, providing invaluable insights into the underlying molecular and neurological mechanisms, tightly controlling LSD-specific pathologies and therapeutic-treatment responses.

Supplementary Material: The following supporting information can be downloaded at: https://www.mdpi.com/article/doi/s1; **Figure S1**. Structural alignment of Gaucher disease-related proteins; **Figure S2**. Structural alignment of Fabry disease-related proteins; **Figure S3**. Structural alignment of Niemann-Pick disease type C1- and C2-related proteins; **Figure S4**. Structural alignment of Tay-Sachs and Sandhoff disease-associated proteins; **Figure S5**. Structural alignment of proteins related to Pompe disease; **Figure S6**. Structural alignment of Hurler syndrome-associated proteins; **Figure S7**. Structural alignment of Hunter syndrome-related proteins; **Figure S8**. Structural alignment of Sly disease-associated proteins; **Table S1**: Gene-specific, DNA oligonucleotide, primers, used in this study.

Author Contributions: ***Conceptualization***, D.J.S.; ***Methodology***, A.D.V.; ***Software***, A.D.V.; ***Validation***, S.P.M., A.D.V. and D.J.S.; ***Formal Analysis***, S.P.M., N.-J.K., Z.C., S.K., A.D.V. and D.J.S.; ***Investigation***, S.P.M., N.-J.K., Z.C., S.K., A.D.V. and D.J.S.; ***Resources***, A.D.V. and D.J.S.; ***Data Curation***, S.P.M., A.D.V. and D.J.S.; ***Writing—Original Draft Preparation***, A.D.V.; ***Writing—Review and Editing***, D.J.S.; ***Visualization***, S.P.M., A.D.V. and D.J.S.; ***Supervision***, A.D.V. and D.J.S.; ***Project Administration***, A.D.V. and D.J.S. All authors have read and agreed to the published version of the manuscript.

Funding: This research received no external funding.

Informed Consent Statement: Not applicable.

Data Availability Statement: The original contributions presented in this study are included in the Original Article/Supplementary Material. Further inquiries can be directed at the Corresponding Authors.

Acknowledgements: The -transgenic- fly stocks, used in this study, were obtained from the Bloomington *Drosophila* Stock Center (BDSC) (NIH P40OD018537) (Indiana, USA). S.P.M. acknowledges financial support from the "Bodossaki Foundation", through its 51st Scholarship Program for Postgraduate and Doctoral Studies (Academic Year: 2023-2024).

Conflicts of Interest: The authors declare no conflicts of interest.

References

1. Parenti, G.; Andria, G.; Ballabio, A. Lysosomal storage diseases: from pathophysiology to therapy. *Annu Rev Med* **2015**, *66*, 471–486, doi:10.1146/annurev-med-122313-085916.
2. Fuller, M.; Meikle, P.J.; Hopwood, J.J. Epidemiology of lysosomal storage diseases: an overview. In *Fabry Disease: Perspectives from 5 Years of FOS*, Mehta, A., Beck, M., Sunder-Plassmann, G., Eds.; Oxford, 2006.
3. Meikle, P.J.; Hopwood, J.J.; Clague, A.E.; Carey, W.F. Prevalence of lysosomal storage disorders. *JAMA* **1999**, *281*, 249–254, doi:10.1001/jama.281.3.249.
4. Platt, F.M.; d'Azzo, A.; Davidson, B.L.; Neufeld, E.F.; Tifft, C.J. Lysosomal storage diseases. *Nat Rev Dis Primers* **2018**, *4*, 27, doi:10.1038/s41572-018-0025-4.
5. Seranova, E.; Connolly, K.J.; Zatyka, M.; Rosenstock, T.R.; Barrett, T.; Tuxworth, R.I.; Sarkar, S. Dysregulation of autophagy as a common mechanism in lysosomal storage diseases. *Essays Biochem.* **2017**, *61*, 733–749, doi:10.1042/EBC20170055.
6. van Gool, R.; Tucker-Bartley, A.; Yang, E.; Todd, N.; Guenther, F.; Goodlett, B.; Al-Hertani, W.; Bodamer, O.A.; Upadhyay, J. Targeting neurological abnormalities in lysosomal storage diseases. *Trends Pharmacol Sci* **2022**, *43*, 495–509, doi:10.1016/j.tips.2021.11.005.

7. Marques, A.R.A.; Saftig, P. Lysosomal storage disorders - challenges, concepts and avenues for therapy: beyond rare diseases. *J Cell Sci* **2019**, *132*, doi:10.1242/jcs.221739.
8. Parkinson-Lawrence, E.J.; Shandala, T.; Prodoehl, M.; Plew, R.; Borlace, G.N.; Brooks, D.A. Lysosomal storage disease: revealing lysosomal function and physiology. *Physiology (Bethesda)* **2010**, *25*, 102–115, doi:10.1152/physiol.00041.2009.
9. Ozkara, H.A. Recent advances in the biochemistry and genetics of sphingolipidoses. *Brain Dev* **2004**, *26*, 497–505, doi:10.1016/j.braindev.2004.01.005.
10. Kolter, T.; Sandhoff, K. Sphingolipid metabolism diseases. *Biochim Biophys Acta* **2006**, *1758*, 2057–2079, doi:10.1016/j.bbamem.2006.05.027.
11. Myerowitz, R. Tay-Sachs disease-causing mutations and neutral polymorphisms in the Hex A gene. *Hum Mutat* **1997**, *9*, 195–208, doi:10.1002/(SICI)1098-1004(1997)9:3<195::AID-HUMU1>3.0.CO;2-7.
12. Pfrieger, F.W. The Niemann-Pick type diseases - A synopsis of inborn errors in sphingolipid and cholesterol metabolism. *Prog Lipid Res* **2023**, *90*, 101225, doi:10.1016/j.plipres.2023.101225.
13. Kubaski, F.; de Oliveira Poswar, F.; Michelin-Tirelli, K.; Matte, U.D.S.; Horovitz, D.D.; Barth, A.L.; Baldo, G.; Vairo, F.; Giugliani, R. Mucopolysaccharidosis Type I. *Diagnostics (Basel)* **2020**, *10*, doi:10.3390/diagnostics10030161.
14. Correa, T.; Feltes, B.C.; Giugliani, R.; Matte, U. Disruption of morphogenic and growth pathways in lysosomal storage diseases. *WIREs Mech Dis* **2021**, *13*, e1521, doi:10.1002/wsbm.1521.
15. Bellen, H.J.; Wangler, M.F.; Yamamoto, S. The fruit fly at the interface of diagnosis and pathogenic mechanisms of rare and common human diseases. *Hum Mol Genet* **2019**, *28*, R207–R214, doi:10.1093/hmg/ddz135.
16. Rigon, L.; De Filippis, C.; Napoli, B.; Tomanin, R.; Orso, G. Exploiting the Potential of Drosophila Models in Lysosomal Storage Disorders: Pathological Mechanisms and Drug Discovery. *Biomedicines* **2021**, *9*, doi:10.3390/biomedicines9030268.
17. Zhang, T.; Peterson, R.T. Modeling Lysosomal Storage Diseases in the Zebrafish. *Front Mol Biosci* **2020**, *7*, 82, doi:10.3389/fmolb.2020.00082.
18. Denton, D.; Shravage, B.; Simin, R.; Mills, K.; Berry, D.L.; Baehrecke, E.H.; Kumar, S. Autophagy, not apoptosis, is essential for midgut cell death in Drosophila. *Curr Biol* **2009**, *19*, 1741–1746, doi:10.1016/j.cub.2009.08.042.
19. Livak, K.J.; Schmittgen, T.D. Analysis of relative gene expression data using real-time quantitative PCR and the 2(-Delta Delta C(T)) Method. *Methods* **2001**, *25*, 402–408, doi:10.1006/meth.2001.1262.
20. Jumper, J.; Evans, R.; Pritzel, A.; Green, T.; Figurnov, M.; Ronneberger, O.; Tunyasuvunakool, K.; Bates, R.; Zidek, A.; Potapenko, A.; et al. Highly accurate protein structure prediction with AlphaFold. *Nature* **2021**, *596*, 583–589, doi:10.1038/s41586-021-03819-2.
21. Varadi, M.; Anyango, S.; Deshpande, M.; Nair, S.; Natassia, C.; Yordanova, G.; Yuan, D.; Stroe, O.; Wood, G.; Laydon, A.; et al. AlphaFold Protein Structure Database: massively expanding the structural coverage of protein-sequence space with high-accuracy models. *Nucleic Acids Res* **2022**, *50*, D439–D444, doi:10.1093/nar/gkab1061.
22. EMBL-EBI. AlphaFold Protein Structure Database. Available online: https://alphafold.ebi.ac.uk (accessed on 21-11-2024).
23. Schrodinger, LLC. The PyMOL Molecular Graphics System, Version 2.0. **2015**.
24. Reva, B.A.; Finkelstein, A.V.; Skolnick, J. What is the probability of a chance prediction of a protein structure with an rmsd of 6 A? *Fold. Des.* **1998**, *3*, 141–147, doi:10.1016/s1359-0278(98)00019-4.
25. Hu, Y.; Flockhart, I.; Vinayagam, A.; Bergwitz, C.; Berger, B.; Perrimon, N.; Mohr, S.E. An integrative approach to ortholog prediction for disease-focused and other functional studies. *BMC Bioinformatics* **2011**, *12*, 357, doi:10.1186/1471-2105-12-357.
26. Hu, Y.; Comjean, A.; Rodiger, J.; Liu, Y.; Gao, Y.; Chung, V.; Zirin, J.; Perrimon, N.; Mohr, S.E. FlyRNAi.org-the database of the Drosophila RNAi screening center and transgenic RNAi project: 2021 update. *Nucleic Acids Res* **2021**, *49*, D908–D915, doi:10.1093/nar/gkaa936.

27. Dietzl, G.; Chen, D.; Schnorrer, F.; Su, K.C.; Barinova, Y.; Fellner, M.; Gasser, B.; Kinsey, K.; Oppel, S.; Scheiblauer, S.; et al. A genome-wide transgenic RNAi library for conditional gene inactivation in Drosophila. *Nature* **2007**, *448*, 151–156, doi:10.1038/nature05954.
28. Brand, A.H.; Perrimon, N. Targeted gene expression as a means of altering cell fates and generating dominant phenotypes. *Development* **1993**, *118*, 401–415.
29. Katarachia, S.A.; Markaki, S.P.; Velentzas, A.D.; Stravopodis, D.J. Genetic Targeting of dSAMTOR, A Negative dTORC1 Regulator, during Drosophila Aging: A Tissue-Specific Pathology. *Int J Mol Sci* **2023**, *24*, doi:10.3390/ijms24119676.
30. Schrodinger, LLC. The PyMOL Molecular Graphics System, Version 1.8. **2015**.
31. Bier, E. Drosophila, the golden bug, emerges as a tool for human genetics. *Nat Rev Genet* **2005**, *6*, 9–23, doi:10.1038/nrg1503.
32. McGuire, S.E.; Roman, G.; Davis, R.L. Gene expression systems in Drosophila: a synthesis of time and space. *Trends Genet* **2004**, *20*, 384–391, doi:10.1016/j.tig.2004.06.012.
33. Southall, T.D.; Elliott, D.A.; Brand, A.H. The GAL4 System: A Versatile Toolkit for Gene Expression in Drosophila. *CSH Protoc* **2008**, *2008*, pdb top49, doi:10.1101/pdb.top49.
34. Farfel-Becker, T.; Vitner, E.B.; Futerman, A.H. Animal models for Gaucher disease research. *Dis. Model. Mech.* **2011**, *4*, 746–752, doi:10.1242/dmm.008185.
35. Kawasaki, H.; Suzuki, T.; Ito, K.; Takahara, T.; Goto-Inoue, N.; Setou, M.; Sakata, K.; Ishida, N. Minos-insertion mutant of the Drosophila GBA gene homologue showed abnormal phenotypes of climbing ability, sleep and life span with accumulation of hydroxy-glucocerebroside. *Gene* **2017**, *614*, 49–55, doi:10.1016/j.gene.2017.03.004.
36. Krause, S.A.; Overend, G.; Dow, J.A.T.; Leader, D.P. FlyAtlas 2 in 2022: enhancements to the Drosophila melanogaster expression atlas. *Nucleic Acids Res* **2022**, *50*, D1010–D1015, doi:10.1093/nar/gkab971.
37. Lakocevic, M.B.; Platisa, M.M.; Sumarac, Z.R.; Suvajdzic, N.D.; Macukanovic, L.D.; Petakov, M.S. Peripheral neural response and sex hormones in type 1 Gaucher disease. *J Med Biochem* **2020**, *39*, 60–65, doi:10.2478/jomb-2019-0020.
38. Vuolo, D.; Do Nascimento, C.C.; D'Almeida, V. Reproduction in Animal Models of Lysosomal Storage Diseases: A Scoping Review. *Front Mol Biosci* **2021**, *8*, 773384, doi:10.3389/fmolb.2021.773384.
39. Meijon-Ortigueira, M.D.M.; Solares, I.; Munoz-Delgado, C.; Stanescu, S.; Morado, M.; Pascual-Izquierdo, C.; Villalon Blanco, L.; Belanger Quintana, A.; Menendez-Conde, C.P.; Morales-Conejo, M.; et al. Women with Gaucher Disease. *Biomedicines* **2024**, *12*, doi:10.3390/biomedicines12030579.
40. Lucchesi, J.C.; Kuroda, M.I. Dosage compensation in Drosophila. *Cold Spring Harbor perspectives in biology* **2015**, *7*, doi:10.1101/cshperspect.a019398.
41. Ohshima, T.; Murray, G.J.; Swaim, W.D.; Longenecker, G.; Quirk, J.M.; Cardarelli, C.O.; Sugimoto, Y.; Pastan, I.; Gottesman, M.M.; Brady, R.O.; et al. alpha-Galactosidase A deficient mice: a model of Fabry disease. *Proc Natl Acad Sci U S A* **1997**, *94*, 2540–2544, doi:10.1073/pnas.94.6.2540.
42. Braunstein, H.; Papazian, M.; Maor, G.; Lukas, J.; Rolfs, A.; Horowitz, M. Misfolding of Lysosomal alpha-Galactosidase a in a Fly Model and Its Alleviation by the Pharmacological Chaperone Migalastat. *Int J Mol Sci* **2020**, *21*, doi:10.3390/ijms21197397.
43. Huang, X.; Suyama, K.; Buchanan, J.; Zhu, A.J.; Scott, M.P. A Drosophila model of the Niemann-Pick type C lysosome storage disease: dnpc1a is required for molting and sterol homeostasis. *Development* **2005**, *132*, 5115–5124, doi:10.1242/dev.02079.
44. Cattaneo, F.; Pasini, M.E.; Intra, J.; Matsumoto, M.; Briani, F.; Hoshi, M.; Perotti, M.E. Identification and expression analysis of Drosophila melanogaster genes encoding beta-hexosaminidases of the sperm plasma membrane. *Glycobiology* **2006**, *16*, 786–800, doi:10.1093/glycob/cwl007.
45. Leonard, R.; Rendic, D.; Rabouille, C.; Wilson, I.B.; Preat, T.; Altmann, F. The Drosophila fused lobes gene encodes an N-acetylglucosaminidase involved in N-glycan processing. *J Biol Chem* **2006**, *281*, 4867–4875, doi:10.1074/jbc.M511023200.
46. De Filippis, C.; Napoli, B.; Rigon, L.; Guarato, G.; Bauer, R.; Tomanin, R.; Orso, G. Drosophila D-idua Reduction Mimics Mucopolysaccharidosis Type I Disease-Related Phenotypes. *Cells* **2021**, *11*, doi:10.3390/cells11010129.

 doi:10.20944/preprints202511.1571.v1

47. Rigon, L.; Kucharowski, N.; Eckardt, F.; Bauer, R. Modeling Mucopolysaccharidosis Type II in the Fruit Fly by Using the RNA Interference Approach. *Life (Basel)* **2020**, *10*, doi:10.3390/life10110263.
48. Bar, S.; Prasad, M.; Datta, R. Neuromuscular degeneration and locomotor deficit in a Drosophila model of mucopolysaccharidosis VII is attenuated by treatment with resveratrol. *Dis. Model. Mech.* **2018**, *11*, doi:10.1242/dmm.036954.